DAVID BAQAEE
University of California, Los Angeles

MICHAEL MINA
Harvard University

EMMANUEL FARHI
Harvard University

JAMES H. STOCK
Harvard University

Policies for a Second Wave

ABSTRACT In the spring of 2020, the initial surge of COVID-19 infections and deaths was flattened using a combination of economic shutdowns and noneconomic non-pharmaceutical interventions (NPIs). The possibility of a second wave of infections and deaths raises the question of what interventions can be used to significantly reduce deaths while supporting, not preventing, economic recovery. We use a five-age epidemiological model combined with sixty-six-sector economic accounting to examine policies to avert and to respond to a second wave. We find that a second round of economic shutdowns alone are neither sufficient nor necessary to avert or quell a second wave. In contrast, noneconomic NPIs, such as wearing masks and personal distancing, increasing testing and quarantine, reintroducing restrictions on social and recreational gatherings, and enhancing protections for the elderly together can mitigate a second wave while leaving room for an economic recovery.

Beginning the third week of March 2020, much of the US economy shut down in response to the rapidly spreading novel coronavirus and rising death rates from COVID-19. The shutdown triggered the sharpest and deepest recession in the postwar period, with just under 30 million new claims for unemployment insurance filed in the six weeks starting March 15. The economic shutdown, combined with other non-pharmaceutical interventions (NPIs), slowed and then reversed the national weekly death rate and brought estimates of the effective reproductive number of the epidemic

Conflict of Interest Disclosure: The authors did not receive financial support from any firm or person for this paper or from any firm or person with a financial or political interest in this paper. They are currently not officers, directors, or board members of any organization with an interest in this paper. No outside party had the right to review this paper before circulation. The views expressed in this paper are those of the authors and do not necessarily reflect those of Harvard University or the University of California, Los Angeles.

to one or less in nearly all states.[1] With the epidemic seemingly under control, state authorities, urged on by a White House eager to resume normal economic activity, began relaxing both economic and noneconomic restrictions. Some of the least hard-hit states started reopening in late April or early May, while others waited until late May or June. As of the date of this conference (June 25), however, the weekly number of confirmed cases is rising nationally, especially outside the Northeast, raising the specter of a second wave of deaths. If countered by a second round of economic shutdowns, short-term unemployment could become long-term and firms could close, dimming prospects for a robust post-COVID-19 recovery.

This paper examines policy options for avoiding or mitigating a second wave of deaths and economic shutdowns. To do so, we use a combined epidemiological-economic model that permits considerable granularity in NPIs. We distinguish between economic NPIs, which directly constrain economic activity (such as closing certain sectors), and noneconomic NPIs, which do not (such as wearing masks and personal distancing).

Our main finding is that a second wave can be avoided or, if it starts, turned around through the use of noneconomic NPIs, avoiding the need for a second round of economic shutdowns. Effective noneconomic NPIs include personal distancing and the wearing of masks; limits on sizes of group activities, especially indoors; increased testing and quarantine; and enhancing protections for the elderly. There is strong evidence that much of the decline in economic activity was the result of self-protective behavior by individuals, not government shutdown orders, so simply reversing those orders will not by itself revive the economy. By using noneconomic NPIs, not only can shutdown orders be avoided but, at least as importantly, a declining trend in deaths will reassure workers that it is safe to return to the workplace and consumers that it is safe to return to shops and restaurants.

Strengthening noneconomic NPIs requires a combination of government guidance and financial support, compliance by firms and retail establishments, and public acceptance and adoption. Like others, we find that increased testing and quarantine can be particularly effective in reducing the circulating pool of contagious individuals. But increased testing requires wider availability of tests, faster turnaround, and reduced test costs. Similarly, additional protections for the elderly, such as regular

1. See, for example, the estimates on R_t COVID-19, https://rt.live/.

testing of staff and residents in nursing homes—who to date account for an estimated 41 percent of COVID-19 deaths (Kaiser Family Foundation 2020)—require more than just guidelines and mandates to ensure that long-term care facilities have the institutional capacity to test and to handle the resulting staffing fluctuations. Wearing masks and maintaining personal distancing requires leadership and education at all levels of government and, at the level of the individual, a desire not to be the reason someone else gets sick. Each of these NPIs is imperfect but together they can reduce the probability of transmission sufficiently to make room for people to return to working, shopping, and eating out, even if a second wave reemerges.

Our main findings are illustrated in figure 1, which shows our baseline second wave scenario, and in figure 2, which examines the effectiveness of tackling the second wave by an economic lockdown versus tackling it using noneconomic NPIs while keeping the economy largely open. Each figure shows simulated weekly US deaths, actual deaths (through June 25), and the monthly unemployment rate. The bands represent statistical estimation uncertainty. Figure 1 (bottom) shows quarterly GDP, although for brevity GDP is not shown in subsequent figures. The simulation period begins on June 1 (vertical dashed line). As described in section VI, in this second wave scenario noneconomic restrictions such as social distancing, wearing masks, religious gatherings, and limits on group sizes at social and sports events are relaxed to be roughly halfway between their restrictive values of mid-May and their prepandemic values of February 2020. In reality, during the shutdown and reopening, economic activity is determined by a complex interaction between policymakers regulating business openings and individuals choosing to shop and work; we model this by a decision maker ("governor") who expands or contracts economic activity in response to economic conditions and deaths using a rule based on guidance from the Centers for Disease Control and Prevention (CDC). In response to rising deaths, in the second wave scenario in figure 1 the governor recloses some businesses, and the unemployment rate rises to the mid-teens early in the fall, leading to a *W*-shaped recession. By the end of the year, there will have been 482,000 deaths, and GDP remains roughly 5 percent below its peak in 2019:Q4.

The top panel of figure 2 examines whether the governor-cum-citizens could avoid this scenario through a second economic lockdown with severity comparable to April. In short, no: simply closing businesses, unaccompanied by noneconomic NPIs, reduces year-end deaths to 410,000 but does

Figure 1. Second Wave from Relaxed Social Distancing and Early Reopening: Weekly Deaths, the Unemployment Rate, and GDP

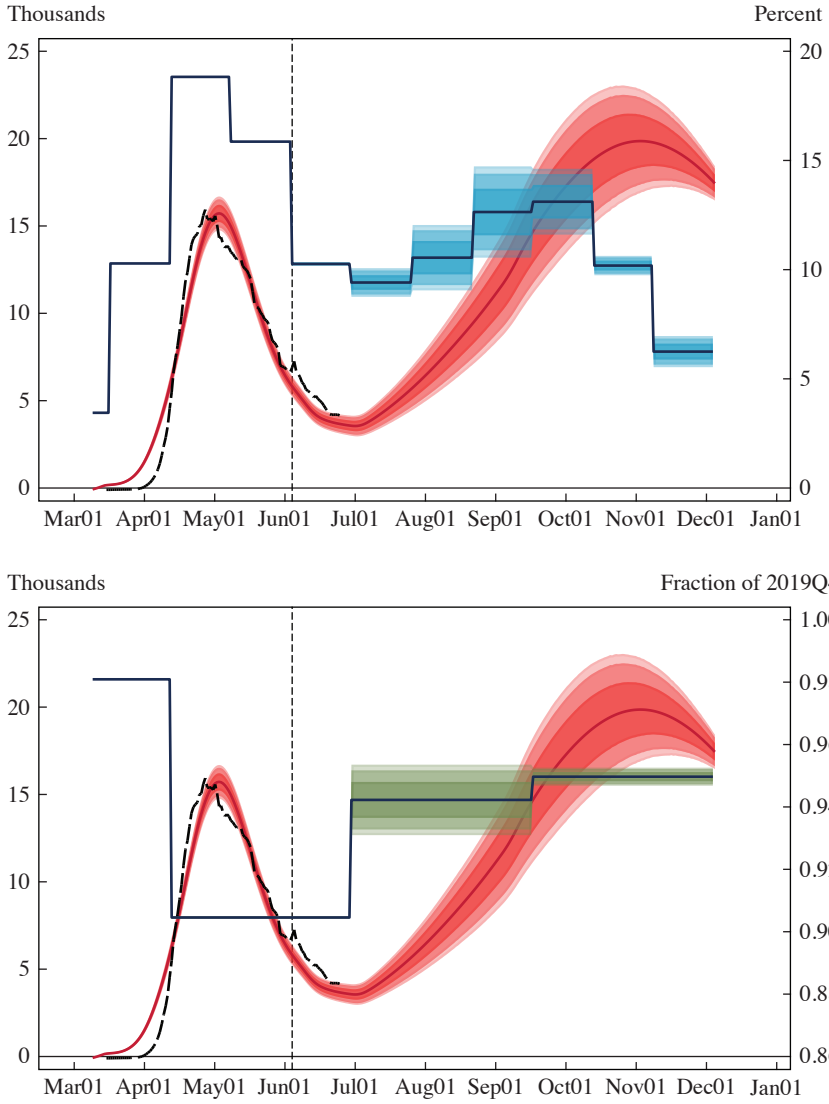

Source: Authors' calculations.

Notes: Each chart shows the level of weekly COVID-19 deaths, actual (dashed) and simulated. The top panel shows the unemployment rate (measured by hours lost) and the bottom panel shows the level of quarterly GDP, indexed to February 2020 = 1. Bands denote +/– 1, 1.65, and 1.96 standard deviations arising from sampling uncertainty for the estimated parameters. The population-wide IFR is 0.7 percent. Total deaths on January 1: 482,000. Simulation begins on June 1 (vertical dashed line).

Figure 2. Responding to the Second Wave: Deaths and Unemployment Rates

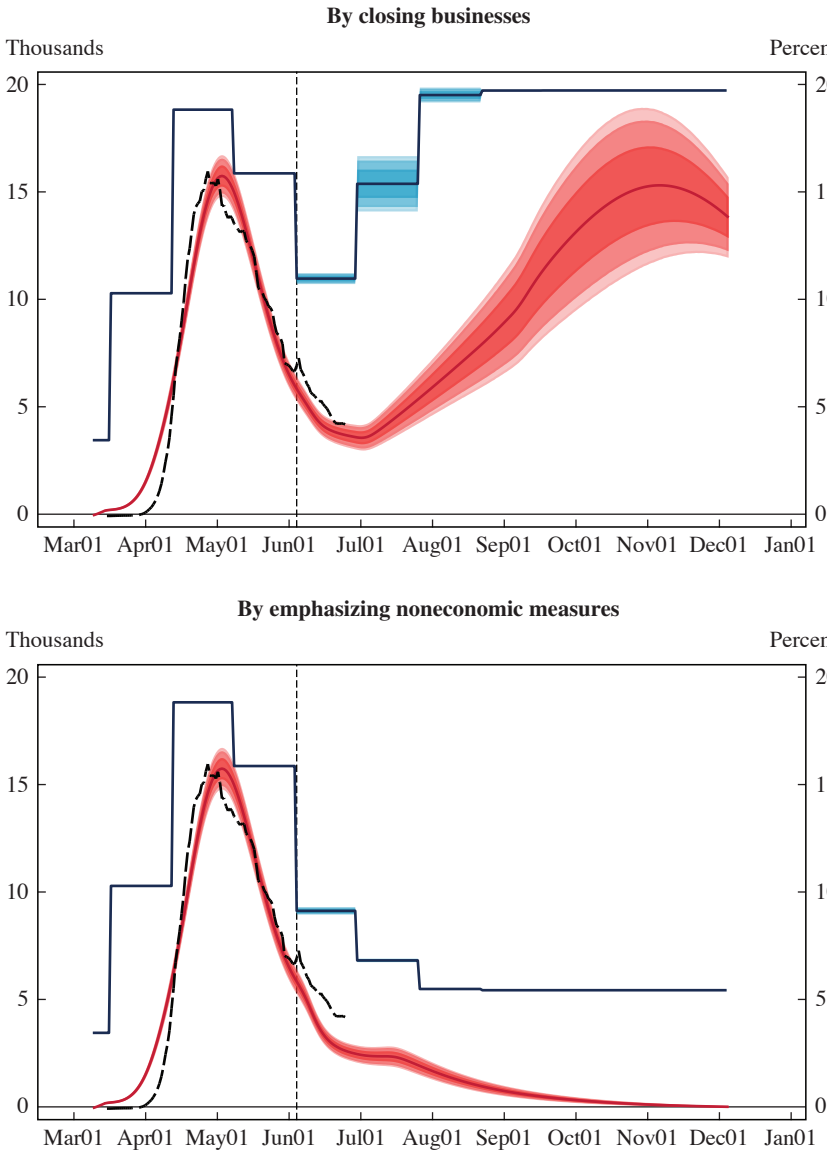

Source: Authors' calculations.

Notes: Both panels show weekly deaths and the monthly unemployment rate. Total deaths on January 1: 410,000 (top) and 147,000 (bottom). Bands denote +/– 1, 1.65, and 1.96 standard deviations arising from sampling uncertainty for the estimated parameters.

not prevent the second wave, at the cost of a vast increase in the unemployment rate. The main reason for this finding is that (as discussed in section II), among workers, contacts at the workplace account for only one-half of all their contacts; in our second wave scenario, the main driver of infections is contacts in nonwork activities, where protections like social distancing and wearing masks have been relaxed.

In contrast, as shown in the bottom panel of figure 2, noneconomic NPIs—including wearing masks, social distancing, limits on social group sizes, protections for the elderly, an achievably higher level of testing, and quarantine—combined with judicious use of economic NPIs like requiring workers who can work from home to continue to do so, eliminate the second wave. In this scenario, the decline in deaths allows the economy to return to near-normal levels of employment. Our modeling suggests that a second wave can be reversed through the adoption of noneconomic NPIs without needing to close either schools or the economy.

Relative to the fast reopening in figure 1, the smart reopening in figure 2 (bottom panel) saves 335,000 lives. Relative to the second shutdown in figure 2 (top panel), the smart reopening increases GDP in the second half of 2020 by $115 billion and reduces the year-end unemployment rate by 14 percentage points.[2]

RELATED LITERATURE Our model combines epidemiological and economic components at a level of granularity that allows us to consider NPIs that vary by age (such as school closings) and across economic sectors (such as reopenings staggered by sector). The epidemiological component is an age-based susceptible-infected-recovered (SIR) model with five age bins, mortality rates that vary by age, and exposed and quarantined components, which we combine with a sixty-six-sector economic model.

2. Subsequent to the conference, as of the time of this writing (July 17), the national death rate started to rise again, led by states that reopened early without requiring noneconomic NPIs. Currently orders to wear masks and to limit large-group gatherings are being resisted by the public and some officials in some states, and in some cases are being litigated. The second wave/shutdown scenario in figure 2 (top panel) therefore currently appears to be the most likely of these three. The smart reopening simulation in figure 2 (bottom panel) would in particular have required earlier and more widespread wearing of masks, more testing, and more restrictions on high-risk noneconomic activity (bars, crowded beaches, mass events) than actually occurred, and currently actual deaths are on track to surpass, by the end of July, the year-end death total in the smart reopening simulation. Of course, the value of these noneconomic NPIs does not expire, and politicians and the public still could choose to transition to a low-death, high-economic-activity path like that in figure 2 (bottom panel).

There is a rapidly growing literature that merges epidemiological and economic modeling to undertake policy analysis for the pandemic.[3] Although most of the models in the literature are highly stylized, they provide useful qualitative guidance.

Broadly speaking, this literature provides six main lessons. First, for a virus with a high fatality rate like SARS-CoV-2, the optimal policy is to take aggressive action early to drive prevalence nearly to zero (Alvarez, Argente, and Lippi 2020; Jones, Philippon, and Venkateswaran 2020; Farboodi, Jarosch, and Shimer 2020); doing so not only decreases the costs from deaths but also provides an environment in which endogenously self-protecting individuals choose to return to economic activity. Second, testing combined with quarantine has high value and reduces the need for a severe economic lockdown (Alvarez, Argente, and Lippi 2020; Berger, Herkenhoff, and Mongey 2020; Eichenbaum, Rebelo, and Trabant 2020b). Third, because deaths are highest among the elderly, focusing resources on protecting older workers or the most vulnerable can provide large benefits (Acemoglu and others 2020; Rampini 2020). Fourth, noneconomic NPIs such as masks and social distancing can reduce both economic costs and deaths (Bodenstein, Corsetti, and Guerrieri 2020; Farboodi, Jarosch, and Shimer 2020). Fifth, nuanced economic NPIs, for example, with sectoral or age variation, can facilitate a quicker reopening (Azzimonti and others 2020; Favero, Ichino, and Rustichini 2020; Glover and others 2020). Sixth, a common theme through these papers is that individual self-protective behavior both anticipates and reduces the effect of regulatory interventions like lockdowns, although because of the contagion and other externalities, individual response alone is typically less than socially optimal.

Our modeling underscores many of these conclusions. Additionally, we are able to examine the interactions among various NPIs in a setting that is carefully calibrated to epidemiological parameters and to current US conditions, allowing direct comparisons of the various NPIs.

3. See Acemoglu and others (2020), Alvarez, Argente, and Lippi (2020), Atkeson (2020a, 2020b), Aum, Lee, and Shin (2020), Azzimonti and others (2020), Baqaee and Farhi (2020a, 2020b), Berger, Herkenhoff, and Mongey (2020), Bodenstein, Corsetti, and Guerrieri (2020), Budish (2020), Eichenbaum, Rebelo, and Trabant (2020a, 2020b), Farboodi, Jarosch, and Shimer (2020), Favero, Ichino, and Rustichini (2020), Glover and others (2020), Guerrieri and others (2020), Jones, Philippon, and Venkateswaran (2020), Krueger, Uhlig, and Xie (2020), Lin and Meissner (2020), Ludvigson, Ma, and Ng (2020), Morris and others (2020), Moser and Yared (2020), Mulligan (2020), Rampini (2020), Rio-Chanona and others (2020), and Stock (2020).

Additional pertinent literature estimates the extent to which the economic contraction starting in March was an endogenous response to the virus or a direct causal consequence of government strictures. This question is a topic of papers in this volume by Bartik and others (2020) and by Gupta, Simon, and Wing (2020), so we refer the reader to their discussion of this literature.

CAVEATS Our results require three important caveats. First, while our sixty-six-sector model provides considerable granularity, some of the highest-risk economic activities, such as nightclubs and attendance at indoor professional sports, are subsectors within our sixty-six sectors. Because we do not model those highest-contact activities directly, we exclude them from our general conclusion that the economy can be reopened safely by relying on noneconomic NPIs. Prudence suggests that this tail of highest-risk activities, which account for a small fraction of economic activity, should remain closed, perhaps until there is a vaccine. Second, our national model misses the regional heterogeneity of the pandemic. Third, although we have taken pains to include the best available estimates for calibrating the model, much about the pandemic remains uncertain, and the confidence bands in the simulation figures understate actual considerable uncertainty (this uncertainty is explored in the online appendix).

I. The Model

We use an age-based SIR model with exposed and quarantined compartments and with age-specific contact rates. An age-based approach matters for four reasons. First, death rates vary sharply by age. Second, workplace shutdowns affect working-age members of the population. Third, different industries have different age structures of workers, so reopening policies that differentially affect different industries could have consequences for death rates as a result of the death-age gradient. Fourth, some policies affect different ages differently, such as closing and reopening schools and only allowing workers of a certain age to return to their workplace.

I.A. Age-Based SEIQRD Model

The model simplifies Towers and Feng (2012) and follows Hay and others (2020), adding a quarantined compartment. We consider five age groups: ages 0–19, 20–44, 45–64, 65–74, and 75+. The epidemiological state variables are S (susceptible), E (exposed), I (infected), Q (quarantined), R (recovered), and D (dead). The state variables are all five-dimensional vectors, with each element an age group, so for example I_2 is the number

of infected who are ages 20–44. The unit of time is daily. We assume that the recovered are immune until a vaccine or effective treatment becomes available.[4]

Let S_a (etc.) denote the ath element of S (ath age group). The SEIQRD model is:

$$dS_a = -\beta S_a \sum\nolimits_b \rho_{ab} C_{ab} \left(\frac{I_b}{N_b} \right) \tag{1}$$

$$dE_a = -dS_a - \sigma E_a \tag{2}$$

$$dI_a = \sigma E_a - \gamma I_a - \delta_a I_a - \chi I_a \tag{3}$$

$$dQ_a = \chi I_a - \gamma Q_a - \delta_a Q_a \tag{4}$$

$$dR_a = \gamma I_a + \gamma Q_a \tag{5}$$

$$dD_a = \delta_a I_a + \delta_a Q_a \tag{6}$$

The total number of individuals of age a is $N_a = S_a + E_a + I_a + Q_a + R_a$.

The parameters of the model are the adult transmission rate β, the recovery rate γ, the latency rate σ, the age-dependent death rate δ_a, the quarantine rate χ, the 5×5 contact matrix C (with element C_{ab}), and age-dependent transmission factors ρ_{ab}. The adult transmission rate β reflects the probability of an adult becoming infected from a close contact with an infected adult. The factors ρ_{ab} allow for transmission rates involving children to differ from the adult-adult rate; ρ_{ab} is normalized to be 1 for adult-adult contacts. Transmission can be mitigated by protective measures such as masks. As discussed below, we model those protective measures separately and accordingly define β to be the transmission rate without mitigation, so that β is determined by the biology of the disease and preexisting social customs (e.g., hand shaking). The latency rate σ and the recovery rate γ are biological characteristics of the disease. The death

4. The assumption of subsequent immunity among the recovered is a matter of ongoing scientific investigation. A working hypothesis based on the related coronaviruses causing MERS and SARS is that immunity could decay but last for one to three years. Because our simulations run through the end of 2020, our assumption is that the recovered are immune through that period.

rate δ_a varies by age. The parameter χ is the removal rate into quarantine, the value of which depends on quarantine policy. Calibration and estimation of the model is discussed in section IV.

The contact matrix C is the mean number of contacts among different age groups in the population. Thus, according to equations (1) and (2), a susceptible adult of age a who comes into contact with an adult of age b has an instantaneous infection probability of β times the probability that the age-b adult is infected. The total instantaneous probability of infection is the sum over the expected transmission by contacts of different ages if those contacts are infected, times the probability that the contacted individual is infected.

In the model, an infected individual is placed into quarantine with some probability, at which point they no longer can infect others. In practice, identifying the infected individual requires testing, contact tracing, or both. In addition, in the United States, quarantine is imperfect and amounts to encouragement to self-isolate. The model abstracts from these complexities.

Other than the quarantine rate χ, the parameters in the model represent preexisting conditions at the start of the epidemic. Policy and self-protective behavior can be thought of as either changing the values of these parameters or, alternatively, introducing additional parameters in the model. For example, the probability of transmission from a contact is reduced substantially if both individuals are wearing masks. In addition, lockdown orders and self-limiting behavior can reduce the number and ages of contacts, that is, alter the elements of the contact matrix. Our modeling of such NPIs, both self-protective and mandated, is discussed in section III.

In a model without quarantine and with transmission rates and death rates that depend on age, the initial reproduction number R_0 is

$$R_0 = \beta \,\text{maxRe}\left[\text{eval}\left(\tilde{C} \bullet \Gamma\right)\right], \tag{7}$$

where maxRe[eval(.)] denotes the maximum of the real part of the eigenvalues of the matrix argument, $\tilde{C}$ is the normalized contact matrix with elements $\tilde{C}_{ab} = \left(\frac{C_{ab}N_a}{N_b}\right)$, $\Gamma_{ab} = \rho_{ab}/(\gamma + \delta_b)$, and $\bullet$ is the element-wise product.[5] Equation (7) generalizes the familiar expression for R_0 in a scalar

5. Equation (7) is derived using the next-generation matrix method; see Towers and Feng (2012) and van den Driessche (2017).

SIR model ($R_0 = \beta/(\gamma + \delta)$) to age-based contacts with age-dependent transmission and death rates.[6]

I.B. Sector- and Activity-Based Contact Matrices

The contact matrix C represents the expected number of contacts in a day between individuals in different age bins. We distinguish between contacts made in three activities: at home, at work (on the work site), and other. Other includes both contacts made as a consumer engaging in economic activity, such as shopping, air travel, or dining at a restaurant, and in noneconomic activities, such as free recreation and social events. In a given day, an individual can be in one, two, or all three of these three states.

The expected number of contacts made in a day is the sum of the contacts made at home conditional on being at home, plus those made at work conditional on being at work, plus those made while engaged in other activities conditional on doing other activities, times the respective probabilities of being in those three states. To differentiate between work in different sectors, which among other things differs by the degree of personal proximity and numbers of contacts at the workplace, we further distinguish work contacts by sector. Accordingly, the expected number of contacts at work is the weighted average of the expected number of contacts, conditional on working in sector i, times the probability of working in sector i. Thus,

$$C_{ab} = p_a^{home} C_{ab}^{home} + p_a^{other} C_{ab}^{other} + \sum_{sectors\, i} p_{a,i}^{work} C_{ab,i}^{work}, \tag{8}$$

where C_{ab}^{home} is the (a, b) element of the contact matrix conditional on being at home, p_a^{home} is the probability of an age-a individual being at home, similarly for other, $C_{ab,i}^{work}$ is the (a, b) element of the contact matrix conditional on being at work in sector i, and $p_{a,i}^{work}$ is the probability of an age-a individual working in sector i, that is, the employment share of sector i as a fraction of the population. That is, let $L_{a,i}$ be the number of workers of age a employed in sector i; then,

$$p_{a,i}^{work} = \frac{L_{a,i}}{N_a}. \tag{9}$$

6. The parameter β differs in the scalar and age-based settings, where β in the scalar model is the transmission rate β in the age-based model times the expected number of contacts.

The disaggregation of the contact matrices in equation (8) distinguishes between different types of contacts. A server in a restaurant has contact with a customer in his or her capacity as a worker (work contact matrix for restaurants), while customers will have contact with the server in their capacity as consumers engaged in an other activity. Similarly, a home health aide providing services to an elderly person at the client's home will be in contact with the elderly person as part of work, while the elderly client will be making that contact at home.

I.C. Employment, Unemployment, and Output

Employment by age, by sector, and total (L) are respectively sums over sectors, ages, and overall. Let the subscript • denote summation over that index. Then,

$$L_{a,\bullet} = \sum_{\text{sectors } i} L_{a,i},\ L_{\bullet,i} = \sum_{\text{ages } a} L_{a,i}, \text{ and } L = \sum_{a} L_{a,\bullet} = \sum_{i} L_{\bullet,i}. \tag{10}$$

The departure of output from its full-employment level is estimated using Hulten's (1978) theorem, which says that the elasticity of real GDP to the total hours worked in a given sector is given by the total labor income in this sector, Ψ_i, as a share of nominal GDP:

$$d\ ln\ Y = \sum_{\text{sectors } i} \Psi_i d\ ln\ L_{\bullet,i}. \tag{11}$$

We discuss this approximation further in section VI.C.

In the counterfactual simulations, labor supply is constrained in two ways. First, if schools are closed, a fraction of workers will not have other child-care options so will be unable to return to work. Second, the virus reduces labor supply because some workers are temporarily quarantined and some have died.

II. Data Sources

We briefly summarize the data used to calibrate the model and historical NPIs, with details provided in the online appendix.

II.A. Economic Data

Employment by age and industry are estimated using the 2017 American Community Survey.

An important NPI is reducing workplace density by having workers work at home. Using data from the Real-Time Population Survey, Bick,

Blandin, and Mertens (2020) estimate that 35.2 percent of the workforce worked entirely from home in May 2020, up from 8.2 percent in February. We use the fraction of workers working from home from their Real-Time Population Survey to estimate the fraction of workers working from home in February and at the end of May. We construct a daily time series of the national fraction working from home by interpolating and extrapolating these points using the national Google workplace visit mobility index.[7] This aggregate time series is apportioned to the sector level using Dingel and Neiman's (2020) estimates of the (prepandemic) fraction of workers in an occupation who can work from home, reported to the sixty-six input-output sectors classification using a crosswalk.

Mongey, Pilossoph, and Weinberg (2020) construct an index of high personal proximity (HPP) by occupation, which measures an occupation as HPP if it is above the median value of proximity as measured by within-arm's-length interactions by occupation. This occupational index was cross-walked to the sixty-six sectors.

Daily sectoral shocks to labor shares by industry are estimated from hours reductions reported in the February–June monthly establishment survey (tables B1, broken down to the sectoral level proportionally to the sectoral employment changes reported in table B2).[8] These provide the estimates of the sectoral shocks to hours for the establishment survey reference weeks. Between the reference weeks, the sectoral shocks were linearly interpolated, and extrapolated after the June reference week, using the Google workplace visit mobility index.

Data on workers' child-care obligations are from Dingel, Patterson, and Vavra (2020).

II.B. Contact Matrices and Epidemiological Data

The contact matrices are estimated using POLYMOD contact survey data.[9] Conditional contact matrices for home, work, and other were computed by sampling contact matrices from the POLYMOD survey data and then reweighting them to match US demographics on these three activities.

7. Google COVID-19 Community Mobility Reports, https://www.google.com/covid19/mobility/.

8. Establishment survey data can be found at the Bureau of Labor Statistics, "Labor Force Statistics from the Current Population Survey," https://www.bls.gov/cps/.

9. POLYMOD Social Contact Data, https://doi.org/10.5281/zenodo.1157934), version 1.1 (2017).

We used the age distribution of workers by industry and Mongey, Pilossoph, and Weinberg's (2020) personal proximity index, cross-walked to the sector level (HPP_i), to construct industry-specific conditional contact matrices, $C_{ab,i}^{work}$ as the product of HPP_i times the overall conditional mean contact matrix, with all sectoral matrices scaled so that the weighted mean equals the overall mean work contact matrix.[10]

The probabilities p^{other} in equation (8) are estimated from the POLYMOD contact data (normalized for US demographics). The probability p^{home} is nearly 1 in the POLYMOD diaries (i.e., nearly everyone spends part of their day at home) and is set to 1 for all simulations.

Daily death data, which are used to estimate selected model parameters, are from the Johns Hopkins COVID-19 GitHub repository.[11]

II.C. Calibration of Historical NPIs

We use an index of nonwork Google mobility data and school closing data to estimate the historical pattern of reduction in nonwork, nonhome (other) activities and thus other contacts. We refer to these generally as historical NPIs, some of which are a consequence of government decisions (e.g., closing schools) and some of which represent voluntary self-protection. We construct a Google mobility index (GMI) using three Google mobility measures at the daily level (national averages): retail and recreation, transit stations, and grocery and pharmacies. These three measures are averaged, normalized so that 1 represents the mean of the final two weeks of February 2020, and smoothed (centered seven-day moving average). Dates of school closings are taken from Kaiser Family Foundation (2020), aggregated to the national level using population weighting. Section IV explains the use of these data to create time-varying contact matrices.

II.D. Epidemiological Parameters

We reviewed twenty papers with medical estimates of incubation periods and duration of the disease once symptomatic (see the online appendix). These papers provided twenty-three estimates of the incubation

10. As an alternative, we sampled from the POLYMOD contact diary data to compute the conditional distribution (element-wise) for at-work contacts and sampled from the 15th, 50th, and 85th percentiles to construct low, median, and high conditional contact matrices, then assigned an industry to one of these three groups based on its HPP value. This approach yielded similar contact matrices by sector to the first approach and behaved similarly in simulations.

11. JHU CSSE COVID-19 Dataset, https://github.com/CSSEGISandData/COVID-19/tree/master/csse_covid_19_data.

(the latency) period and sixteen estimates of the period from becoming symptomatic to being recovered (the recovery period). For the latency period, we used the mean value from the three peer-reviewed studies with estimates, which yields a latency period of 4.87 days and a value of $\sigma = 1/4.87$ (continuous-time, daily time scale). For the recovery period, the studies have very long estimates, from 17.5 to 28.3 days, which appear to reflect sample selection in the studies which tend to consider the most severe (and longest-lasting) cases. Estimates of the recovery period used in the epidemiological literature are shorter, and we use Kissler and others' (2020) estimate of an infectious period of five days. As a sensitivity check, we also consider an infectious period of nine days; as shown in the online appendix, our simulation results are not sensitive to this change so the analysis in the text uses the five-day recovery period.

Salje and others (2020) and Verity and others (2020) provide estimates of the infection-fatality ratio (IFR) by age. Ferguson and others (2020) adjust Verity and others' (2020) IFRs to account for nonuniform attack rates across ages. Salje and others (2020) use data from France and the *Diamond Princess* cruise ship; they have lower IFRs at the youngest ages and slightly higher IFRs at the older ages than Ferguson and others (2020). We adopt the more recent IFR profile from Salje and others (2020), scaled proportionately to match a specified overall (population-wide) IFR.[12] The overall IFR is not known because of insufficient random population testing. We therefore adopt a range of estimates of the population IFR from 0.4 percent to 1.1 percent; the age-specific IFR is then obtained using Salje and others' (2020) IFR age profile. The population-wide IFR is weakly identified in our model. For our main results we use a population-wide IFR of 0.7 percent and report sensitivity analysis in the online appendix.

Boast, Munro, and Goldstein (2020) and Vogel and Couzin-Frankel (2020) provide largely nonquantitative surveys of the sparse literature concerning transmissibility of the virus in contacts involving children. To calibrate the parameters ρ_{ab} involving children, we reviewed nine studies on this topic posted between February 21 and May 1. These studies point to a lower transmission rate for contacts involving children, although the estimates vary widely. Of the seven studies that estimate a transmission rate from children to adults, our mean estimate, weighted by study relevance, is $\rho_{1b} = 0.44$, $b > 1$. Of the four studies that estimate transmission

12. Specifically, our vector of age-IFRs in percentages is $c(0.001, 0.020, 0.28, 1.35, 7.18)$, where c is set to yield the indicated population IFR (0.6 percent in our base case).

rates from adults to children, our weighted mean estimate is $\rho_{a1} = 0.27$, $a > 1$. We are unaware of estimates of child-child transmission rates so, lacking data, we set ρ_{11} to the average, $\rho_{11} = (\rho_{1b} + \rho_{a1})/2$. These estimates are highly uncertain and some of the simulation results are sensitive to their values; that sensitivity is discussed further in the text and in more detail in the online appendix.

III. GDP-to-Risk Index

One reopening question is whether sectors should be reopened differentially based on either their contribution to the economy or their contribution to risk of contagion. The expressions for R_0 in equation (7) and for output in equation (11) lead directly to an index of contributions of GDP per increment to R_0. Specifically, consider a marginal addition of one more worker of age a returning to the work site in sector i. Then the ratio of the marginal contribution to output, relative to the marginal contribution to R_0, is

$$\frac{d \ln Y / dL_{a,i}}{dR_0 / dL_{a,i}} \propto \frac{\Psi_i / L_i}{\beta d \max \mathrm{Re}\left[eval\left(\tilde{C} \bullet \Gamma\right)\right] / dL_{a,i}} \equiv \theta_i \tag{12}$$

where the numerator does not depend on a because the output expression (11) does not differentiate worker productivity by age.

The derivative in the denominator in equation (12) depends on the contact matrix; however, as is shown in the online appendix, because of the way that $L_{a,i}$ enters C, this dependence on the full contact matrix is numerically small. Thus, while in principle θ_i varies as employment and the other components of the contact matrix vary, in practice this variation in θ_i is small so that the path of θ_i is well approximated by its prepandemic full-employment value. For the simulations that examine sequential industry reopening, we therefore used equation (12) with the derivatives of maxRe[eval($\tilde{C}$)] numerically evaluated at the baseline values of the contact matrix.

Some algebra for a single-age SIR model provides an interpretation of this index in terms of deaths. It is shown in the online appendix that the effective case reproduction rate, $R^{eff} = R_0(S/N)$, can be written as

$$R^{eff} = 1 + \frac{1}{\gamma + \bar{\delta}} \frac{d \ln D}{dt} = 1 + \frac{1}{\gamma + \bar{\delta}} \frac{\ddot{D}}{\dot{D}}, \tag{13}$$

where $\dot{D} = dD/dt$ and $\ddot{D} = d^2D/dt^2$. At the start of the epidemic, when $S/N = 1$, combining expressions (12) and (13) shows that

$$\theta_i = \left(\gamma + \bar{\delta}\right)\frac{d \ln Y / dL_i}{d\left(\ddot{D}/\dot{D}\right)/dL_{a,i}}, \tag{14}$$

where $\bar{\delta}$ is the population-wide death rate; the subscript a is dropped because equation (13) holds for a single-age SIR. Thus, in a single-age version of the model, θ_i is proportional to the ratio of the marginal growth of GDP to the marginal growth of the daily death rate from adding a worker to sector i.

It is tempting to translate θ into a GDP increment per death for a marginal reopening of a sector; however, the alternative formulation in equation (14) shows that such a calculation depends on the state of the pandemic because the denominator is the contribution to the growth rate of daily deaths. If daily deaths are increasing, adding a worker to a sector is costly because it increases the already-exponential growth rate of deaths. The more negative the growth rate of deaths, the smaller the contribution of the additional worker to the total number of deaths. This is a key insight, that the marginal cost of reopening is contained and can be kept small by a combination of sectoral prioritization and, especially, ensuring that noneconomic NPIs are in place to keep $R^{eff} < 1$ during the reopening.

Standardized and Winsorized values of θ are listed in the table in online appendix A for the sixty-six NAICS code private sectors in our model.[13] We refer to this Winsorized/standardized index as the GDP-to-risk index. The highest GDP-to-risk sectors tend to be white-collar industries such as legal services, insurance, and computer design, along with some high-value moderate-risk production sectors such as oil and gas extraction and truck transportation. Moderate GDP-to-risk industries include paper products, forestry and fishing, and utilities. Low GDP-to-risk industries tend to have many low-paid employees who are exposed to high levels of personal

13. The value of θ as defined in equation (12) depends on epidemiological parameters. To a good approximation, standardization eliminates this dependence, except for the ρ_{ab} factors for transmission involving children—the matrix $\Gamma \approx \rho/(\gamma + \bar{\delta})$, where the matrix ρ has elements ρ_{ab}. There are three outlier sectors (legal, management, and finance and investments) which have very high GDP-to-risk measures. It is numerically convenient to Winsorize to handle these outliers, although the conclusions are not sensitive to the Winsorization.

contacts at work, including residential care facilities, food services and drinking places, social assistants, gambling and recreational industries, transit and ground passenger transportation, and educational services.

IV. Calibration of Historical NPIs and Estimation

The historical paths of contact reduction and self-protective measures, which we collectively refer to as historical NPIs, combine calibration using historical daily data and estimation of a small number of parameters to capture the time paths of self-protective measures, such as wearing masks, on which there are limited or no data. Altogether, the model has five free parameters to be estimated: the initial infection rate I_0 as of February 21, the transmission rate β, and three parameters describing the path of NPIs from March 10 through the end of the estimation sample. The model-implied time-varying estimate of R_0 closely tracks a nonparametric estimate of R_0.

IV.A. Time-Varying Historical Contact Matrices and NPIs

The NPIs that were implemented between the second week of March and mid-May include closing schools, personal distancing, prohibiting operation of many businesses and making changes in the workplace to reduce transmission in others, orders against large gatherings, issuing stay-at-home orders in some localities; wearing masks and gloves, and urging self-isolation among those believed to have come in close contact with an infected individual. These NPIs are a mixture of policy interventions and voluntary measures taken by individuals protecting themselves and their families from infection.

These NPIs enter the model in two ways. The first is through the reduction of contacts; for example, working from home or being furloughed or laid off eliminates a worker's contacts at the workplace. The second is through reducing the probability of transmission (β), conditional on having contact with an infected individual; personal distancing and wearing masks falls in this second category. Our approach to producing time-varying contact matrices and β is a mixture of calibration when we have directly relevant data (for example, dates of school closures, mobility measures of nonwork trips, and measures of the number of employed workers and the fraction of those workers working from home) and estimation of the effect of NPIs for which we do not have data, such as personal distancing and the use of masks.

We introduce these NPIs by modifying equation (8) to allow for time-varying contacts and mitigation:

$$C_{ab,t} = [0.8 + 0.2\phi_t]\, p_a^{home} C_{ab}^{home} + \phi_t \lambda_{ab,t}^{other} p_a^{other} C_{ab}^{other} + \phi_t \sum_{sectors\ i} s_{it} \left(1 - \lambda_{wfh,t}\right) p_{a,i}^{work} C_{ab,i}^{work}. \tag{15}$$

As in equation (8), the total contacts made by someone of age a meeting someone of age b at time t is the sum of the contacts made at home, in other activities, and at work. The conditional contact matrices C_{ab}^{home}, C_{ab}^{other}, and $C_{ab,i}^{work}$ and the probabilities p_a^{home}, p_a^{other}, and $p_{a,i}^{work}$ in equation (15) refer to prepandemic contacts and population weights in equation (8). The remaining factors $\lambda_{ab,t}^{other}$, $\lambda_{wfh,t}$, and s_{it} represent measured reductions in contacts, and the factor φ_t captures NPIs that have the effect of reducing transmission conditional on a contact (e.g., masks).

We briefly describe these factors and motivate the structure of equation (15), starting with the second term, contacts made during other activities. The expected number of contacts made by a meeting b is $\lambda_{ab,t}^{other}$ p_a^{other} C_{ab}^{other}. Attending school is an other activity, so for age < 20 we model school closings by letting $\lambda_{ab,t}^{other}$ be linear in the national average fraction of students with schools open on day t, with $\lambda_{ab,t}^{other} = 1$ if all schools are open and $\lambda_{ab,t}^{other} = 0.3$ if all are closed (accounting for nonschool other contacts). For contacts made by adults, we set $\lambda_{ab,t}^{other}$ to the Google mobility index for other activities described in section III.

The factor φ_t represents the reduction in the transmission probability, relative to the unmitigated transmission rate $\beta\rho_{ab}$, resulting from self-protective NPIs, such as personal distancing, hand hygiene, and wearing a mask. Guidance concerning and use of these protective measures evolved over the course of the pandemic. Early in the pandemic, public health guidance stressed hand washing and disinfecting surfaces. Until April 3, the CDC recommended that healthy people wear masks only when taking care of someone ill with COVID-19. On April 3, the CDC changed that guidance to recommend the use of cloth face coverings, and masks were adopted gradually through April into May.[14] For example, New York implemented a mandatory mask order on April 15, Bay Area counties did so on April 22, Illinois on May 1, Massachusetts on May 6. As of early July many states still did not require masks although some businesses in those

14. IHME, "COVID-19 Projections," https://covid19.healthdata.org/united-states-of-america?view=mask-use&tab=trend, accessed December 2020.

states did. There is now considerable evidence that personal distancing and the use of masks are effective in reducing transmission of the virus.[15] Although there are data on mandatory personal distancing measures by state (Kaiser Family Foundation 2020), we are aware of only limited data on the actual mask usage.[16] Lacking such data, we estimate the aggregate effect of those measures through the scalar risk reduction factor φ_t, parameterized using a flexible functional form, specifically, the first two terms in a type-II cosine expansion, constrained so that $0 \leq \varphi_t \leq 1$:

$$\phi_t = \Phi\left\{\begin{array}{l} f_0 + f_1 \cos[\pi(t - s_0 + 1/2)/(T - T_0)] \\ + f_2 \cos[2\pi(t - s_0 + 1/2)/(T - T_0)] \end{array}\right\} \tag{16}$$

where Φ is the cumulative normal distribution. We set the start date of the NPIs, s_0, to be March 10, three days before the declaration of the national emergency, reflecting the short period between the first reported COVID-19 death in the United States on February 29 and the start of the lockdown. The date T denotes the end of the estimation sample. This parameterization introduces three coefficients to be estimated, f_0, f_1, and f_2.

The second term in equation (15) parameterizes contacts made at home. Most but not all contacts at home involve household members. Using the American Time Use Survey, Dorèlien, Ramen, and Swanson (2020) estimate that 85 percent of contacts made at home or in the yard involve household members; however, their total home contacts are fewer than in our contact matrices, especially for children under age 15, for whom they impute contacts. We therefore make a modest adjustment of their estimate and assume that 80 percent of contacts are among household members. Contacts among household members are modeled as unmitigated, with the remaining 20 percent of at-home contacts that are with nonhousehold members mitigated by the factor φ_t.

15. The effect of masks on COVID-19 transmission has been reviewed by Howard and others (2020), who, following Tian and others (2020), suggest that masks reduce the probability of transmission by the factor $(1 - ep_m)^2$, where e is the efficacy of trapping viral particles inside the mask and p_m is the percentage of the population wearing the mask. Chu and others (2020) conducted a meta-analysis of 172 studies (including studies on SARS and MERS) on personal distancing, masks, and eye protection; their overall adjusted estimate is that the use of masks by both parties has a risk reduction factor of 0.15 (0.07 to 0.34); however, they found no randomized mask trials and do not rate the certainty of the effect as high.

16. The COVID Impact Survey (at https://www.covid-impact.org/, accessed July 17) reports results for surveys at two points in time, late April and early June, and indicates an increase in mask usage over that period.

Figure 3. Illustrative Contact Matrices: Baseline, Estimated for April 15, and Counterfactual

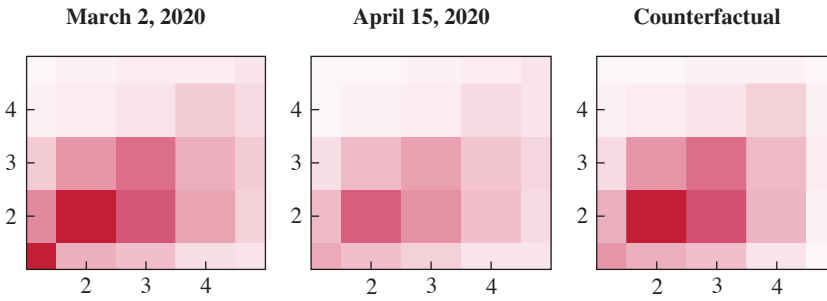

Source: Authors' calculations using POLYMOD data.

Notes: The (a,b) element is the number of contacts made by individual age a (y axis) of individuals of age b (x axis) in a day, for age bins 0–19, 20–44, 45–64, 65–74, and 75+. Darkest indicates eight to nine contacts, lightest indicates less than .2 contacts. From the left, the matrices are the baseline prepandemic contact matrix, the estimated contact matrix as of April 15 (accounting for working at home, layoffs, no school, reduced travel, but not accounting for masks or other transmission-reducing factors), and contacts under a hypothetical in which there is no school, all workers under age 64 return to work, workers 65+ work from home (or not at all), and visits to the elderly are reduced by 75 percent relative to baseline.

The final term in equation (15) parameterizes contacts at work. For workers in sector i, the baseline contacts are reduced by the fraction s_{it} of workers continuing to work,

$$s_{it} = L_{\bullet,i,t}/L_{\bullet,i,t_0}, \tag{17}$$

where $L_{\bullet,i,t}$ is the all-ages labor force in industry i at date t and t_0 is the final week in February 2020. Of those still working, a fraction $\lambda_{wfh,t}$ work from home, leaving the fraction $s_{it}(1 - \lambda_{wfh,t})$ of sector i workers remaining in the workplace. We set s_{it} and $\lambda_{wfh,t}$ equal to, respectively, the daily sectoral shock to the labor share and the time series on the fraction of workers working from home by sector, both of which are described in section II.A. These reduced contacts are then multiplied by the noncontact risk reduction factor φ_t in equation (16).

Figure 3 illustrates three different contact matrices. The first (left) is the baseline prepandemic contact matrix estimated for Monday, March 2. The second (center) is the calibrated contact matrix for Wednesday, April 15, in the midst of the lockdown, constructed using equation (15) with $\varphi_t = 1$, so that the matrix represents only the reduced contacts from school closings, layoffs, working from home, and reduced other activities, not from additional (unmeasured but estimated) protective precautions.

The third matrix is a counterfactual matrix for a scenario considered below, in which workers age 65+ work from home or not at all, other workers return to their workplace, there is no school, and visits to the elderly (including by home health and nursing home workers) are reduced by 75 percent. The effect of these counterfactual adjustments is to reduce contacts in the top row and final column (the oldest age groups), reduce child-child contacts (youngest age group), and for contacts among middle age groups to be similar to baseline levels.

IV.B. Estimation Results

After the calibration described in section IV.A, the SEIQRD model has five free parameters: the initial infection rate I_0, the unrestricted adult transmission rate β, and the three parameters determining φ_t, f_0, f_1, and f_2. These parameters were estimated by nonlinear least squares, fit to the daily seven-day moving average of national COVID-19 deaths from the Johns Hopkins real-time database, using an estimation sample from March 15 to June 12, 2020.[17] The mid-March start of the estimation period is motivated by the evidence of undercounting of COVID-19 deaths, especially early in the epidemic; see, for example, the *New York Times* estimates by Katz, Lu, and Sanger-Katz (2020). This systematic undercounting of deaths provides an important caveat on the parameter estimates; in particular, the initial infection rate could be higher than we estimate.

Table 1 provides estimates of these parameters and their standard errors for selected values of the overall population IFR. Standard errors are reported below the estimates, with the caveat that we are not aware of applicable distribution theory to justify the standard errors given the nonstationary, highly serially correlated data. The final column reports the root-mean-square error (units are thousands of deaths). The only parameter that is independently interpretable outside of the model is the initial number of infections on February 21, I_0, which we estimate to be 3,635 (SE = 370) using our base case population IFR of 0.7 percent.

One overall summary of the fit of the estimated model is the time path of the model-implied effective case reproduction rate, $R^{eff} = R_0(S/N)$. This is plotted in figure 4 over the estimation period (through June 12). The figure also shows a nonparametric estimate computed directly from actual daily

17. Daily deaths have a weekly "seasonal" pattern reflecting weekend effects in reporting. Using the seven-day trailing change in actual and model-predicted deaths smooths over this substantively unimportant noise.

Table 1. Estimated Parameter Values

IFR	$\hat{I}_0$	$\hat{\beta}$	$\hat{f}_0$	$\hat{f}_1$	$\hat{f}_2$	*RMSE*
0.005	4.932	0.051	0.012	0.832	0.804	1.195
	(0.485)	(0.001)	(0.003)	(0.040)	(0.039)	
0.007	3.635	0.050	0.005	0.854	0.821	1.200
	(0.371)	(0.001)	(0.004)	(0.035)	(0.041)	
0.009	2.932	0.0500	0.006	0.879	0.826	1.215
	(0.317)	(0.001)	(0.005)	(0.039)	(0.047)	

Source: Authors' calculations.

Notes: The parameters I_0 and β are, respectively, the initial number of infections on February 21 (in thousands) and the adult transmission rate. The coefficients f_0, f_1, and f_2 parameterize the scaling factor φ_t. Given the infection-fatality ratio (IFR) in the first column and the other model parameters given in the text, the parameters in the table are estimated using data on the seven-day moving average of deaths (in thousands) from March 15 through June 12. Nonlinear least squares standard errors are given in parentheses.

Figure 4. Model-Implied and Nonparametric Estimates of R^{eff}

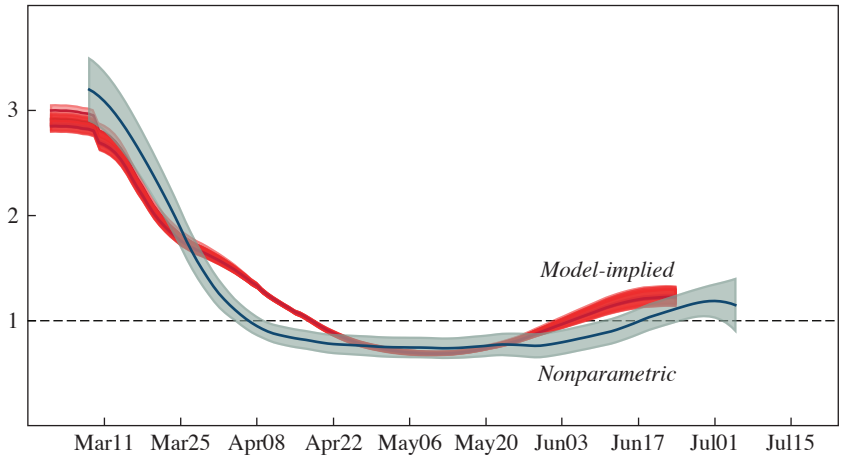

Source: Authors' calculations.

Notes: Ninety-five percent confidence bands shown. The model-implied estimate (dark gray) is computed from the estimated model, for population IFRs = 0.4–1.1 percent. The nonparametric estimate (light gray) is computed using equation (13) with the change in deaths estimated over seven days and daily deaths averaged over the week, using a local quadratic smoother. Nonparametric estimate is shifted by fourteen days to approximate the lag from infections to deaths.

deaths using equation (13).[18] Given the nonstandard serial correlation in the data, neither set of confidence intervals would be expected to have the usual 95 percent frequentist coverage. The model-based and nonparametric estimates are quite similar. Both estimate that, early in the pandemic, the initial R_0 was approximately 3.2, which is within the range of other estimates. With the self-protective measures and government-ordered shutdowns, the effective R dropped sharply through March into April and was estimated to be below 1 from mid-April through mid-May. Subsequently, with the reopening and the increased mobility, the model-based effective R rose slightly above 1, although the nonparametric estimate remained just below 1. The estimated values of R^{eff} are plotted for IFRs ranging from 0.4 percent to 1.1 percent; they are nearly the same, indicating that the IFR is not separately identified in the model as discussed by Atkeson (2020b).

V. Control Rules and Simulation Design

Decision making in the coronavirus epidemic has occurred at all levels of society: consumers decide if they feel it is safe to dine out or travel; workers weigh concerns about the safety of returning to work; local officials decide on when to apply for and how to implement reopening; state officials issue closure orders, mandate noneconomic NPIs, and permit reopenings; and federal agencies attempt to provide guidance. We combine these multiple decision makers, private and public, into a single representative decision maker who is averse to both deaths and unemployment. For convenience, we refer to this decision maker as a governor who has primary authority over decisions to shut down and to reopen, but the term "governor" stands in for the actual, more complex, decentralized decision-making process.

V.A. Control Rules

We model reopening decisions as reacting to recent developments with the twin aims of controlling deaths and reopening the economy in mind. In so doing, we treat the governor as following the CDC and White House

18. The growth rate of daily deaths in equation (13) is estimated by the average seven-day change in deaths divided by the seven-day average daily death rate, smoothed using a local quadratic smoother. The nonparametric estimates assume the SIR model. For an alternative estimator of R that does require information on disease-specific dynamics but does not assume a SIR structure, see Cori and others (2013).

reopening guidelines (White House, CDC, and FDA 2020), which advises reopening the economy if there is a downward trajectory of symptoms and cases for fourteen days, along with having adequate medical capacity and health care worker testing. Because of changes in test availability, confirmed cases are a poor measure of total infections, so we use deaths instead of infections but otherwise follow the spirit of the CDC guidelines.

Specifically, we consider a governor who will restrict activity when deaths are rising or high, relax those restrictions when deaths are falling or low, tend to reopen when the unemployment rate is high, and tend to reopen when the cumulative unemployment gap is high. This final tendency reflects increasing pressures on budgets—personal, business, and public—from each additional week of high unemployment and low incomes on top of previous months.

In the jargon of control theory, this amounts to the governor following a proportional-integral-derivative (PID) control rule, in which the feedback depends on current deaths, the fourteen-day change in deaths (declining death rate), the current unemployment rate, and the integral of the unemployment rate. Accordingly, we suppose that the governor follows the linear PID controller,

$$u_t = \kappa_0 + \kappa_{up} U_{t-1} + \kappa_{ui} \int_{t_0}^{t-1} U_s \, ds + \kappa_{dp} D_{t-1} + \kappa_{dd} \dot{D}_{t-1}, \tag{18}$$

where U_t is the unemployment rate ($= 1 - L_t/L_{t0}$), where t_0 is the end of February 2020) and $\dot{D}$ is the death rate. The CDC recommends tracking not the instantaneous derivative of infections (or D) but the change over fourteen days, and deaths are noisy, suggesting some smoothing of D. Similarly, U is unobserved and at best can be estimated with a lag, even using new and continuing claims for unemployment insurance and nonstandard real-time data. For the various terms on the right-hand side of equation (18) we therefore use, in order, the fourteen-day average of the unemployment rate, the cumulative daily unemployment rate since March 7, deaths over the previous two days (these are observed without noise in our model), and the fourteen-day change in the two-day death rate.

The governor decides whether workplaces can reopen and, if so, whether to stagger the reopening across industries using the GDP-to-risk index. Specifically, we consider a sequence of sectoral reopenings as determined by the PID controller, shifted by the GDP-to-risk index:

$$s_{it} = s_{it_R} + \Phi\left(u_t + \kappa_\theta \theta_i\right)\left(1 - s_{it_R}\right), \tag{19}$$

where s_{it} is the workforce in sector i at date t as a fraction of its February value (see equation [17]), t_R is the initial date of the reopening, and Φ is the cumulative Gaussian distribution, which is used to ensure that the controller takes on a value between 0 and 1 (so sectoral relative employment satisfies $s_{itR} \leq s_{it} \leq 1$). The industry shifter $\kappa_\theta \theta_i$ preferences industry i based on its GDP-to-risk index.

Reopening the economy requires not just working but shopping, which is an other activity. In the historical period, the factor $\lambda_{ab,t}^{other}$ for $a > 2$ is set to equal the Google mobility index for other activities. We model this factor as increasing to 1 proportionately to GDP from its value on t_R as the economy reopens, so that full employment corresponds to $\lambda_{ab,t}^{other} = 1$ for $a > 2$.

V.B. Noneconomic NPIs

Noneconomic NPIs are either under the control of the governor (e.g., reopening schools) or are decisions made by individuals that are influenced by the governor (e.g., attending church). Instead of specifying policy rules for these other NPIs, we examine different scenarios in which the governor behaves according to equations (18) and (19) concerning sectoral reopening. For example, one set of choices entails opening up schools, but with protections (which the governor and school districts can mandate); in the context of equation (15), opening schools corresponds to setting $\lambda_{ab,t}^{other} = 1$ for ages < 20, and protective measures at schools correspond to setting $\varphi_t < 1$ for contacts made at school. For adults, we allow for relaxation of protective measures (masks, personal distancing) according to three reopening phases. For age 75+, we consider scenarios in which they are subject to additional restrictions on visits and greater use of protection than in the general population. These stand in for regular testing of nursing home employees, requiring visiting families to gather outside and to wear masks, and so forth.

VI. Simulation Results

All the simulations have the same structure: the governor controls economic reopening according to the control rule in equation (18), given a specified path of noneconomic NPIs. This structure allows us to quantify the interaction between economic and noneconomic NPIs. In our second wave baseline (figure 1), the governor is pro-reopening so exercises a fast reopening. As an alternative, we consider a slower governor who is more willing to shut down the economy a second time.

The environment in which the governor makes these decisions is specified in terms of NPIs, which differ in each scenario. Some of these, like school reopening, are directly under the governor's control, while others, like masks and personal distancing, are individual decisions that can be influenced by state, federal, and local recommendations and education. The baseline is the fast-reopening second wave scenario in figure 1; each scenario is defined by departures from that baseline. All simulations begin on June 1, which approximates the middle of actual state reopenings. Georgia was the first state to reopen most consumer-facing businesses on April 24, while reopening for some of the hardest-hit regions (for example, Massachusetts, Michigan, and New York City) occurred mainly in June.

The multiple public and private reopening road maps (Gottlieb and others 2020; White House, CDC, and FDA 2020; National Governors Association 2020; Conference Board 2020; Romer 2020) generally reopen in phases, where transition to the next phase is determined by public health gating criteria. We follow this framework and relax (or reimpose) non-economic NPIs in three phases. In the reopening baseline, phase I reopening occurs on May 18, phase II reopening occurs on June 8, phase III reopening occurs on July 1. Nursing homes lag by one phase and enter phase III on September 15. These phases are modeled as (1) an increase, in three equal steps, in the number of other and nonhousehold home contacts from before the lockdown to prepandemic conditions, and (2) a relaxation of personal protective measures (masks, personal distancing) from their mid-May values to a value that is higher but still represents considerable reduction in transmission rates, given a contact, relative to unrestricted conditions. In the second wave baseline, the self-protective factor φ rises from its late-May empirical estimate of 0.26 to 0.67. As a calibration using the formula in footnote 12, a factor of 0.67 corresponds to one-quarter of the population using masks that are 75 percent effective for all nonhousehold contacts. In the reopening baseline, workers working at home return to the workplace during phases I–III. The roadmaps and actual reopenings typically prioritize safer sectors, so in our second wave baseline we use equation (19) with $\kappa_\theta = 1$. If primary and elementary schools reopen, they do so on August 24.

In all scenarios, we assume that workplace safety measures remain in place throughout the simulation period at their estimated late-May level, specifically, the within-workplace transmission factor β is reduced by a factor of 0.26. As calibration using the formula in footnote 12, this corresponds to 65 percent of workers wearing a 75 percent effective mask

when in contact with workers or customers, although in practice workplace safety measures would vary by sector.

Each scenario also specifies an effective quarantine rate. The effective quarantine rate is the fraction of infected individuals who, at some point during their infection, enter quarantine. The rate that is achieved in practice reflects a combination of identifying the infected through testing or contact tracing, government policy concerning those who test positive, and individual compliance. Currently, the CDC website advises individuals who test positive or who are symptomatic to self-isolate "as much as possible."[19] We assume a current quarantine rate of 5 percent which, for example, corresponds to 10 percent of the infected restricting their contacts by half. We consider alternatives of higher quarantine rates later in the summer, which in turn hinges on testing and contact tracing becoming more widely available.

All simulations reported here are for a population-wide IFR of 0.7 percent; sensitivity analysis is provided in the online appendix. Uncertainty spreads in the simulation plots are two standard error bands based on the estimation uncertainty for I_0 and β in table 1. All simulations end on January 1, 2021. Details for all scenarios are available in the online appendix, as are sensitivity results for these scenarios that vary the population-wide IFR and epidemiological parameters.

Figure 5 shows total deaths and the share of recovered individuals by age for the baseline second wave scenario in figure 1. Of the 482,000 deaths by January 1, 56 percent are age 75 or older. By January 1, nearly one-quarter of the population has been infected, with those age 20–44 having the highest recovered rate (31 percent) because of their higher rates of contact. Because of the high rate of recovered individuals, the value of R^{eff} in this simulation is just over 1 by January 1.

Results for mortality by age and GDP are given in the online appendix.

VI.A. Economic NPIs

The first economic NPI, shutting down the economy while holding constant the other assumptions of the second wave baseline, is modeled by the slow governor's response, holding constant the other assumptions of the second wave baseline, and is shown in the top panel of figure 2.

19. "What to Do If You Are Sick," Centers for Disease Control and Prevention, https://www.cdc.gov/coronavirus/2019-ncov/if-you-are-sick/steps-when-sick.html?CDC_AA_refVal=https%3A%2F%2Fwww.cdc.gov%2Fcoronavirus%2F2019-ncov%2Fif-you-are-sick%2Fcaring-for-yourself-at-home.html, accessed June 19, 2020.

Figure 5. Deaths and Share of Recovered by Age for the Second Wave Scenario in Figure 1

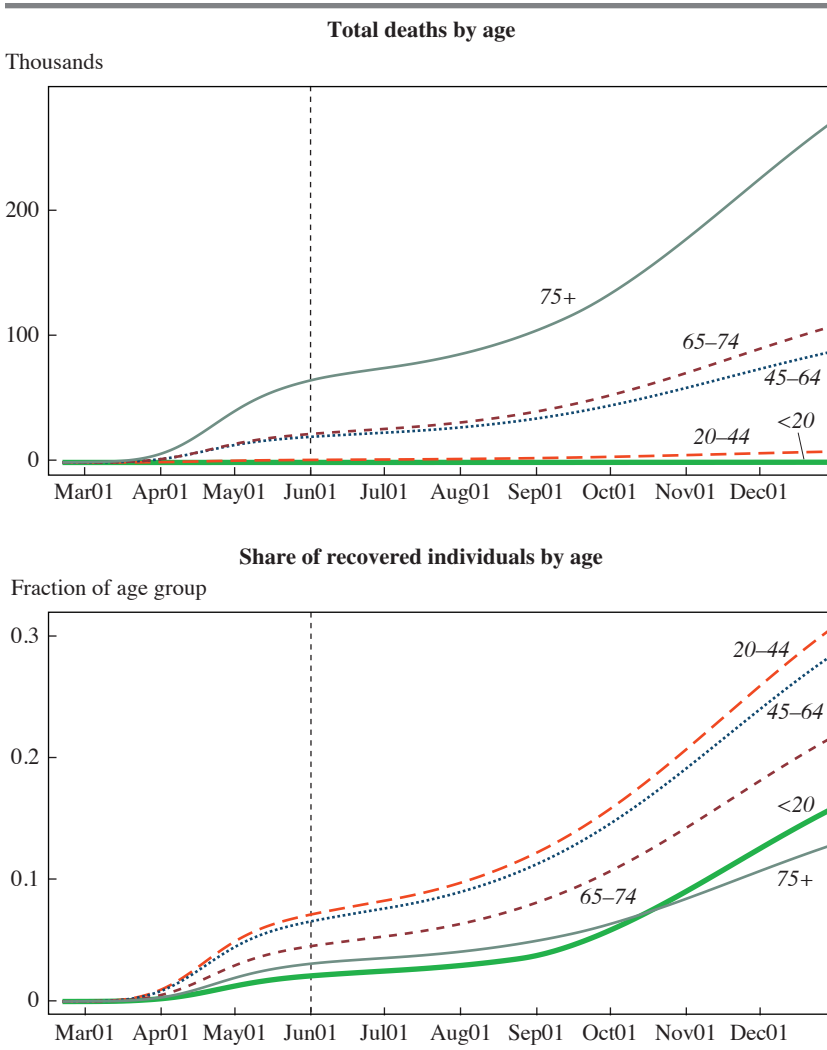

Source: Authors' calculations.

As discussed in the introduction, the second shutdown reduces but does not eliminate the second wave of deaths, while producing rates of unemployment in the mid-teens. Here, we consider the effects of three more-nuanced economic NPIs: relying more heavily on the GDP-to-risk index, so that high-risk, low-value sectors are reopened last and closed first; requiring all workers to work from home; and an age-based policy that requires all workers who are age 65+ to work from home if they can or not to work at all.

The top panel of figure 6 departs from the second wave baseline by implementing a more aggressive sectoral reopening than in figure 1, specifically by increasing κ_θ in equation (19) to $\kappa_\theta = 2$. As it happens, whether one makes more aggressive use of the GDP-to-risk index has a small effect: when the sectoral reopening exploits the GDP-to-risk index, deaths are reduced by 800 and second-half GDP is increased by 0.2 percent (the unemployment rate is very slightly lower under the nuanced reopening because the lower deaths permit a slightly faster reopening). This finding is robust: we have explored the gains from stronger or weaker phasing of reopenings or shutdowns based on the GDP-to-risk index, both Winsorized (used here) and not; while using this index reduces deaths, the gains are modest at best and, in scenarios in which deaths are being brought under control, the benefits of a staged sectoral reopening are nearly negligible. The remaining simulations therefore retain the baseline value of $\kappa_\theta = 1$. Some intuition for the limited benefit of a staged sectoral reopening is that, for the average worker, only half their contacts occur at work, and because workplaces are generally regulated, it is easier to implement and enforce transmission reduction measures at work than in noneconomic other activities such as church or parties; thus the potential gains from staged sectoral reopening are small to begin with.

This finding of small benefits to staggering the sectoral reopening has an important caveat: although our sixty-six sectors provide considerable granularity and exhibit a large variation in the GDP-to-risk index, the sectoral detail does not isolate those few businesses in the highest-risk tail of the contact distribution. For example, NAICS code 722 (food services and drinking places) includes establishments ranging from catering companies to nightclubs. Contacts among customers and workers at high-contact/high transmissibility activities such as nightclubs are in principle in the POLYMOD contact database, so these very high-contact economic activities are in both the workplace and consumption (other activity) components of the model. That said, judgment strongly suggests that such high-contact economic activity would appropriately be treated differently than broad-based reopening: keeping closed the highest-contact economic activities

Figure 6. Economic Non-pharmaceutical Interventions

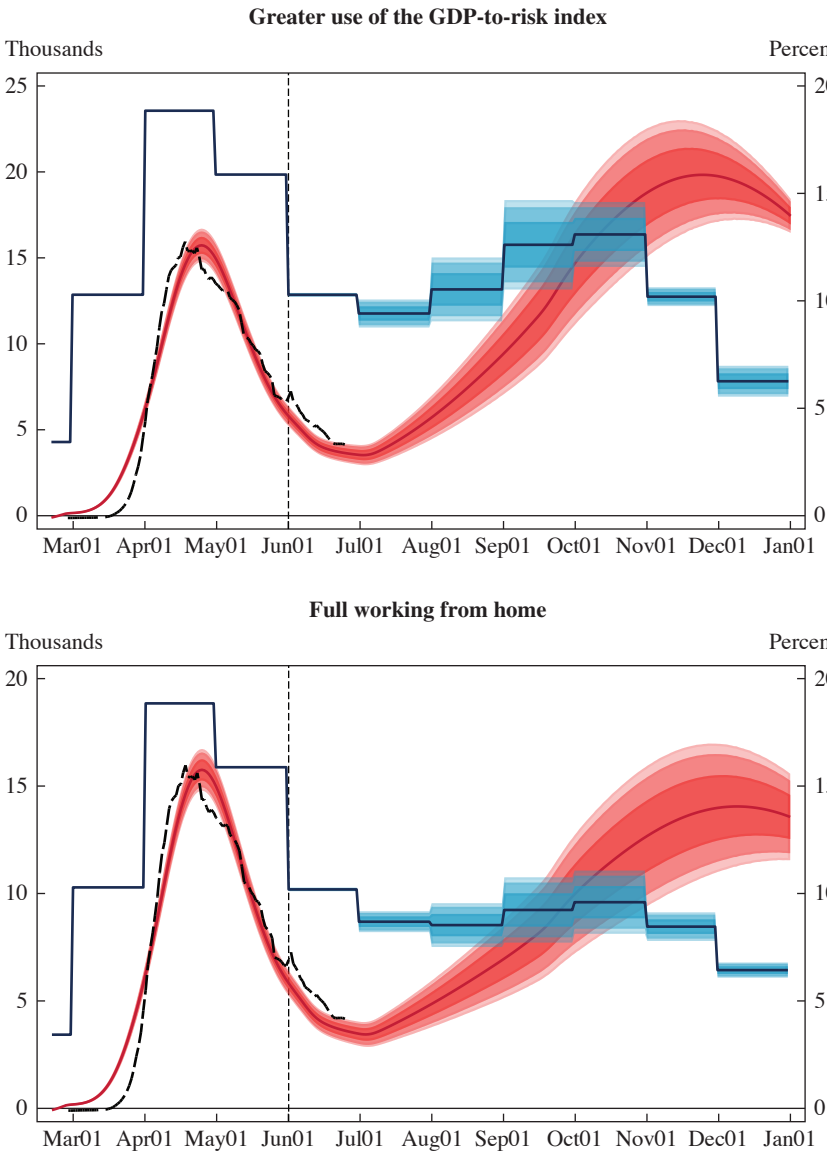

Source: Authors' calculations.

Notes: Baseline is the fast reopening second wave scenario in figure 1. Total deaths by January 1: 482,000 (top) and 383,000 (bottom). Bands denote +/– 1, 1.65, and 1.96 standard deviations arising from sampling uncertainty for the estimated parameters.

could be a justifiable NPI in a cost-benefit sense, perhaps indefinitely until a vaccine is available. These very high-contact activities are a small fraction of economic activity, for example, admissions to movie theaters, sports, and other live entertainment comprised less than 0.6 percent of personal consumption expenditures in 2019.

The bottom panel of figure 6 modifies the second wave baseline by requiring those workers who are able to work from home to continue to do so as businesses reopen. By reducing workplace contacts, this policy reduces deaths by January 1 from 482,000 to 383,000. This reduction in deaths allows the governor to implement a less severe second wave shutdown, so the unemployment rate is lower (by approximately 1 percentage point) during the fall than without the work-from-home order.[20]

Figure 7 (top panel) considers an age-based policy, in which only workers over age 65 are required to work from home, if they are able, or not at all. The effect of this NPI on employment and contagion varies by sector, depending on the age distribution of workers, personal proximity in the workplace, and the extent to which that sector admits working from home. This policy reduces total deaths from 482,000 to 466,000. The year-end unemployment rate is slightly higher under this scenario than the second wave baseline because of the laid-off age 65+ workers.

The bottom panel of figure 7 considers the combined effects of an economic lockdown with these three economic NPIs layered on: leaning more heavily on phasing by sector, requiring working from home, and laying off workers age 65+ who are not able to work from home. These instruments are complementary, and between them they reduce deaths by 171,000. Yet, this full arsenal of economic NPIs neither prevents nor quells the second wave, just limits its damage, and they are accompanied by very high unemployment rates.

Compared to the full shutdown, the three more-nuanced economic NPIs have the virtue of both reducing deaths and supporting overall employment. That said, the main conclusion from these simulations is that the full economic shutdown in figure 2 (top panel), even if combined with the additional economic measures in figures 6 and 7, is not potent enough, by itself, to stop the second wave.

20. We note that there are plausibly effects on productivity from working at home, although a priori the overall sign is unclear. Workers save time commuting; however, they could have distractions such as child care. Bloom and others (2015) find that workers who work from home are more productive; however, that is a pre-COVID-19 study, so there is plausibly selection in those results. See Mas and Pallais (2020) for a review. These potential productivity effects are not included in our calculations.

Figure 7. Economic Non-pharmaceutical Interventions

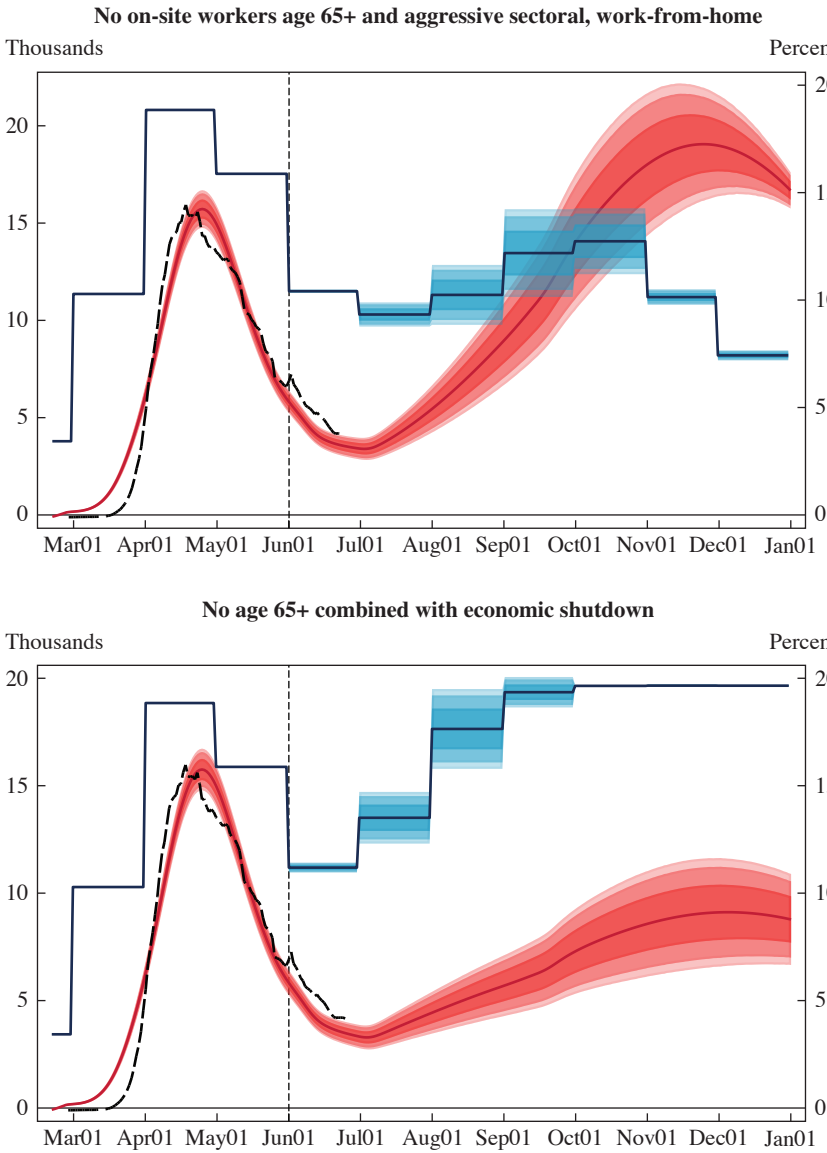

Source: Authors' calculations.

Notes: Baseline is the fast reopening second wave scenario in figure 1. Total deaths by January 1: 466,000 (top) and 311,000 (bottom). Bands denote +/– 1, 1.65, and 1.96 standard deviations arising from sampling uncertainty for the estimated parameters.

VI.B. Noneconomic NPIs

We now turn to four noneconomic NPIs that could mitigate the second wave: not allowing schools to reopen in the fall; undertaking enhanced protections for age 75+, especially the most vulnerable in long-term care facilities; increasing the quarantine rate, which would entail directing resources toward increased testing and contact tracing; and revoking phase III noneconomic relaxation, such as returning to prohibitions on large group gatherings and enhanced mask wearing and personal distancing.

The option of not reopening elementary and secondary schools in the fall is shown in figure 8 (top panel). Not sending children to school reduces contacts among children and between children and their teachers, so reduces the spread of the virus. As discussed in section II, however, contacts involving children are believed to entail lower risk of spreading the virus than contacts among adults, so deaths by January 1 only fall by 26,000. Moreover, if schools are closed, then some workers will be constrained in their labor supply because they must provide child care; as a result, the unemployment rate remains elevated through the fall at just over 10 percent. In addition, closing schools has the undesirable effect of retarding schoolchildren's education, especially for those least able to learn in an online environment. So not reopening schools alone imposes considerable economic and noneconomic costs while not solving the problem of the second wave.

Because COVID-19 mortality rates increase sharply with age, one possible policy is to devote additional resources focused on protecting the elderly. Current CDC guidelines for nursing homes recommend virus testing for all residents and staff but do not specify testing frequency.[21] The CDC also recommends that visitors wear cloth masks and restrict their visit to their relative's room. The Centers for Medicare and Medicaid Services guidelines for reopening long-term care facilities recommend weekly testing of staff, providing staff with personal protective equipment, and delaying outside visitors until the state enters federal phase III reopening.[22] In theory, these are strong and protective steps; however,

21. "Testing Guidelines for Nursing Homes," Centers for Disease Control and Prevention, https://www.cdc.gov/coronavirus/2019-ncov/hcp/nursing-homes-testing.html, accessed June 20, 2020.

22. "Nursing Home Reopening Recommendations for State and Local Officials," Centers for Medicare and Medicaid Services, https://www.cms.gov/medicareprovider-enrollment-and-certificationsurveycertificationgeninfopolicy-and-memos-states-and/nursing-home-reopening-recommendations-state-and-local-officials, accessed May 18, 2020.

Figure 8. Noneconomic Non-pharmaceutical Interventions

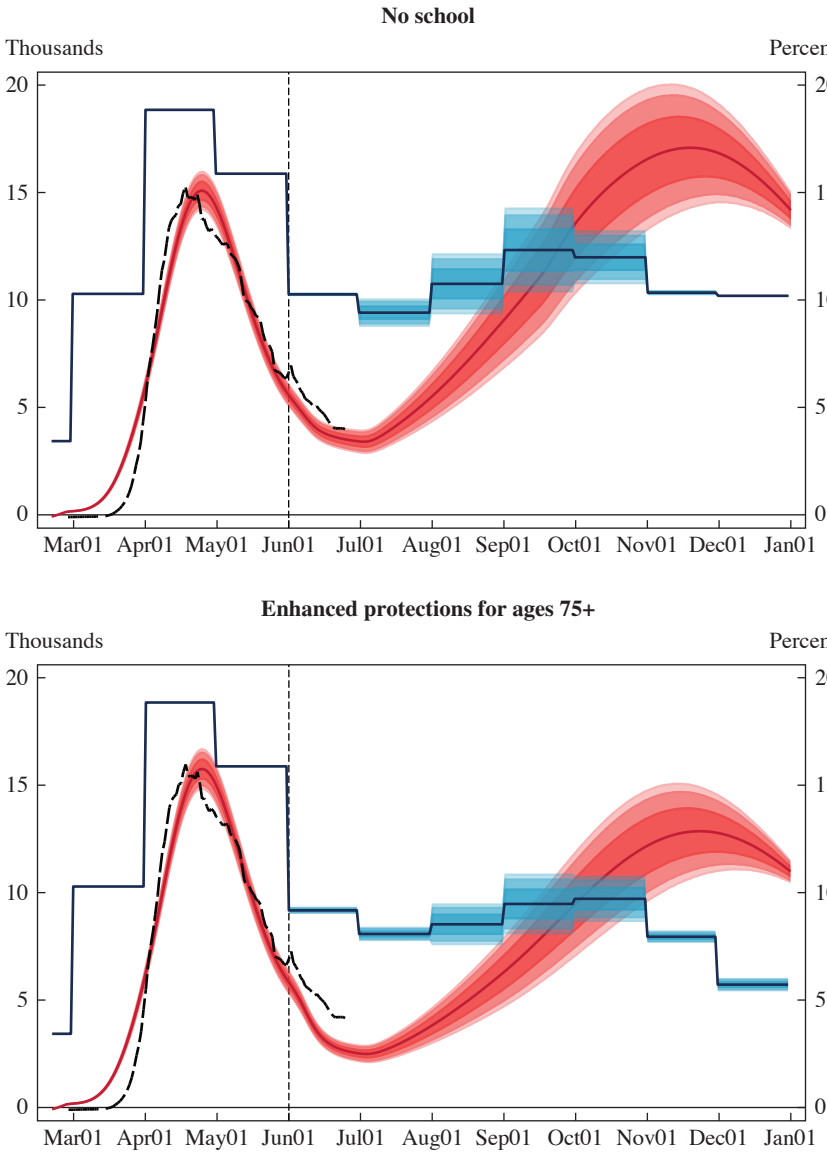

Source: Authors' calculations.

Notes: Baseline is the fast reopening second wave scenario in figure 1. Total deaths by January 1: 456,000 (top) and 355,000 (bottom). Bands denote +/– 1, 1.65, and 1.96 standard deviations arising from sampling uncertainty for the estimated parameters.

it is unclear how the testing and additional staff needed to implement these guidelines will be paid for and whether nursing homes have the institutional capacity to implement these measures.

Figure 8 (bottom panel) examines the effects of enhanced protections for the elderly, modeled as requiring nursing homes to maintain their restrictions on visitors and transmission mitigation measures of late May (the details of how these requirements are met could change in practice, for example, by more staff testing as tests become more available than they were in May). The reduction in deaths is large, by 127,000, about one-third of projected cases under the baseline from July 1 through January 1. This significant saving in life is consistent with the conclusions in Acemoglu and others (2020), although their estimated gains are even larger because they start from a much higher baseline number of deaths. The reduced number of deaths provides room for the governor to be less restrictive and, while under this policy the economy still has a *W*-shaped recession, the second dip is less severe.

The roadmaps generally stress the importance of widespread testing and quarantine. During the spring and summer of 2020, however, testing was notable mainly because of its absence. In some cases, test results were so delayed as to render testing useless for public health purposes. Our enhanced quarantine scenario has a 10 percent effective quarantine rate, that is, 10 percent of infected individuals are sent into perfect quarantine at some point during their infection.[23] Without legally enforceable quarantine, even a 10 percent effective quarantine rate evidently would require a significant increase in testing with fast turnaround, combined with incentives to quarantine. That testing need not be random but instead could be focused on populations who are both at a highest risk of getting the virus and are most likely to spread it.

The effect of a 10 percent quarantine rate (up from 5 percent in the baseline) is shown in the top panel of figure 9; the bottom panel shows results for a 15 percent quarantine rate. Increasing the quarantine rate to 10 percent

23. We consider this effective quarantine rate as ambitious but achievable. Current estimates of the asymptomatic rate vary from less than 40 percent to approximately 80 percent. Yang, Gui, and Xiong (2020) estimate a 42 percent asymptomatic rate for a sample of Wuhan residents. Data in Guðbjartsson and others (2020) suggest a comparable asymptomatic rate in Icelandic testing, and Poletti and others (2020) suggest a 70 percent asymptomatic rate among those younger than 60. As a calibration, suppose that 40 percent of the infected (a high fraction of the symptomatic) get tested, get their results back while they are still infectious, and are advised to self-isolate, that half of those comply, and that those who comply reduce their contacts by 50 percent. This results in a 10 percent effective quarantine rate.

Figure 9. Noneconomic Non-pharmaceutical Interventions

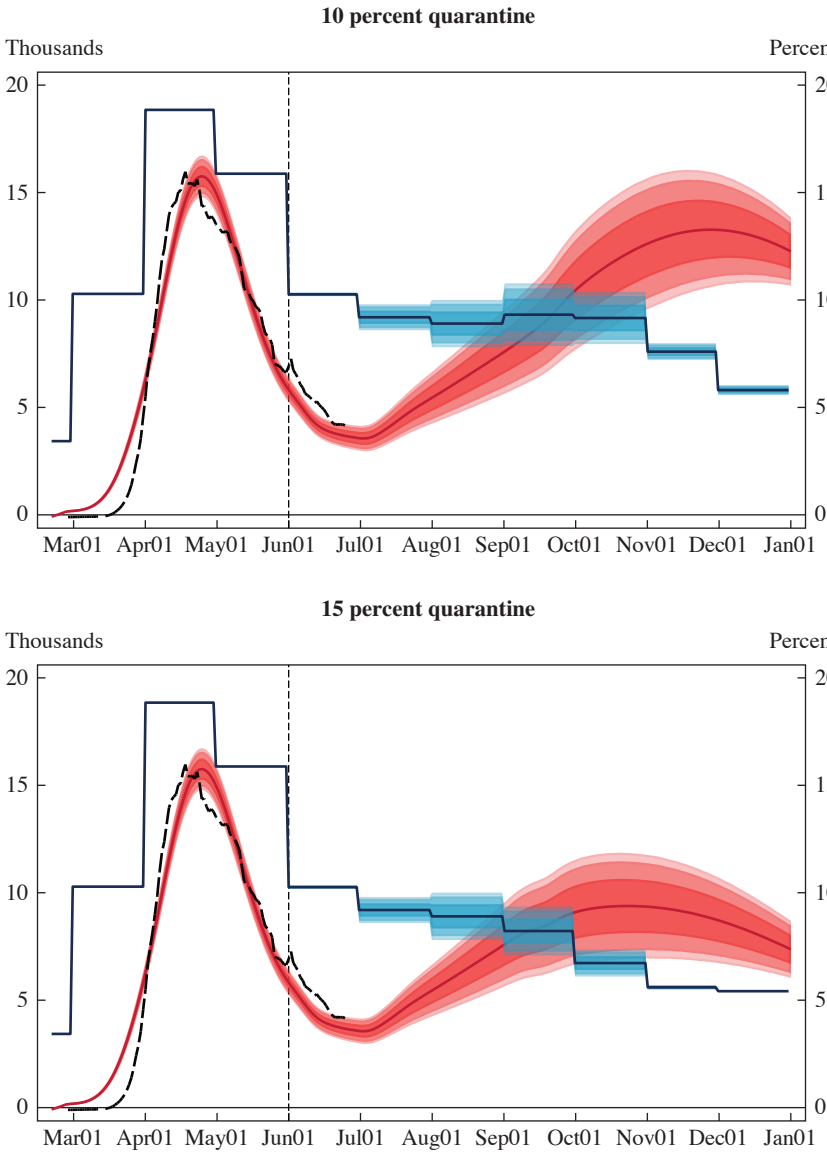

Source: Authors' calculations.

Notes: Baseline is the fast reopening second wave scenario in figure 1. Total deaths by January 1: 384,000 (top) and 331,000 (bottom). Bands denote +/– 1, 1.65, and 1.96 standard deviations arising from sampling uncertainty for the estimated parameters.

reduced fatalities from 482,000 to 384,000 and increasing the quarantine rate to 15 percent nearly flattens the death curve and reduced total deaths to 331,000. With increased testing and quarantine, the governor can pause the economic reopening but does not need a second economic shutdown.

These scenarios all have phased-in lifting of restrictions on noneconomic activities, such as basketball games, large group gatherings, and religious services, as well as partial relaxation of personal protections such as wearing masks. An option available to the governor is to revoke the phase II and III noneconomic reopenings and to call for increased wearing of masks and personal distancing. We therefore consider a case in which the governor reverts to phase I for noneconomic gatherings (church, social, etc.) on July 20, upon seeing the reversal of the previously declining trend in deaths. Recall that phase I noneconomic restrictions are less restrictive than our empirical estimates for mid-May.

Figure 10 (top panel) considers this reversal of noneconomic NPIs. Unlike the imposition of strict economic NPIs or economic shutdowns, this policy brings R^{eff} below 1 and deaths decline: the second wave is kept small and brief. Year-end deaths total only 188,000, and the economy is near full employment.

The final two cases combine some of these noneconomic NPIs. Figure 10 (bottom panel) considers the combined effect of returning to phase I social distancing, enhanced protections for the elderly, and 10 percent quarantine. The combined effect is to reduce year-end deaths to 155,000 with nearly full employment. Figure 2 (bottom panel), discussed in the introduction, additionally requires workers who can to continue to work from home; the result is a further reduction in deaths to 147,000 and nearly full employment throughout the fourth quarter.

VI.C. Cost per Life

A standard approach in the economics literature on the pandemic is to view NPIs through the lens of cost per life saved. There are technical reasons to object to this calculation: standard estimates of the value of life refer to marginal consumption losses whereas the current losses are nonmarginal, and the true cost of a shutdown-induced recession depends on the path of recovery which is highly uncertain.[24] More importantly, the preceding simulations underscore that the value-of-life framing is too narrow for many of these calculations, in which the NPI reduces lives lost *and* improves economic outcomes.

24. See Hall, Jones, and Klenow (2020) for a discussion.

Figure 10. Noneconomic Non-pharmaceutical Interventions: Strong Personal Distancing

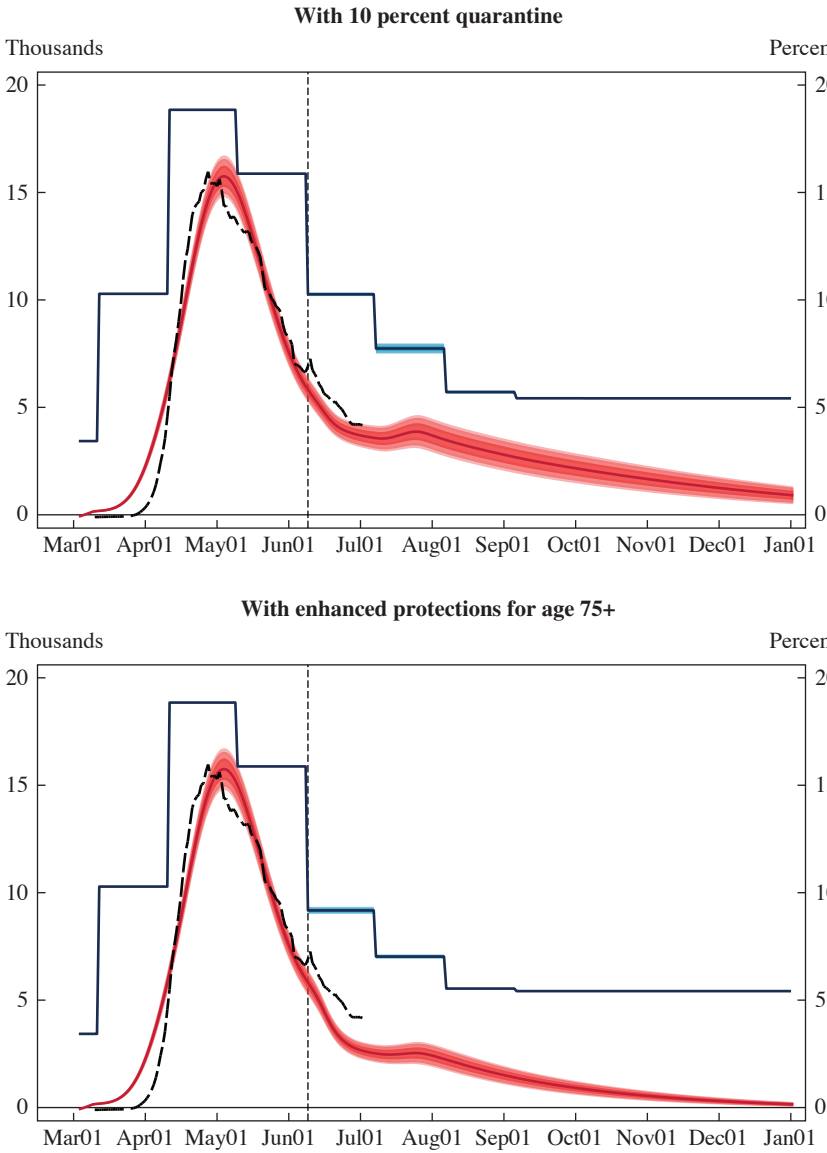

Source: Authors' calculations.

Notes: Baseline is the fast reopening second wave scenario in figure 1. Total deaths by January 1: 188,000 (top) and 155,000 (bottom). Bands denote +/– 1, 1.65, and 1.96 standard deviations arising from sampling uncertainty for the estimated parameters.

With these caveats, one component of a cost-benefit analysis of economic NPIs is the economic cost, measured by lost output, relative to lives saved. The paths of the fast and slow governors allow us to compute the value of lost output per death averted as a result of a slow reopening (or aggressive closing), relative to the fast governor, over the period of the simulation, holding constant all other NPIs.[25] These values vary substantially across NPI scenarios. If an economic lockdown is the only tool used, that is, the scenario in figure 1 versus figure 2 (top panel), the cost per death averted is $11 million. In scenarios with other NPIs, the cost per death averted tends to increase because the other NPIs are reducing deaths, so the marginal value of the lockdown measured in terms of deaths is diminished. For example, if an economic lockdown is layered on top of the reversal in noneconomic NPIs in figure 10 (top panel), the cost per death averted is $24 million. These values exceed typical US government estimates; for example, the US Environmental Protection Agency (2010, appendix B) recommends using $9.1 million (2019 dollars) per death averted.

VI.D. Nonlinear Input-Output Calculations

Our counterfactual GDP estimates use the approximation in equation (11) known as Hulten's (1978) theorem. Hulten's theorem is an equilibrium first-order approximation for small shocks. Given that the sectoral reductions in hours associated with lockdowns are very large, it is natural to question the validity of this approximation. As shown by Baqaee and Farhi (2019, 2020a, 2020b), the quality of the approximation depends on the size of the sectoral shocks and how sectoral labor income shares vary with the shocks, which in turn depends on the elasticities of substitution in consumption and in production. When all the elasticities are equal to one, the economy is Cobb-Douglas, the sectoral labor shares are constant, and Hulten's theorem applies globally and not only as a first-order approximation. However, if the elasticities are less than one, so that there are complementarities, then the quality of the approximation can quickly deteriorate when the shocks get large. This is potentially important given that the empirical literature typically finds that inter-sectoral elasticities are significantly below one.

To gauge the importance of these nonlinearities for our calculations, we consider the counterfactual sectoral reductions in hours in 2020:Q3 in the economic lockdown scenario of figure 2 (top panel). We explore different values within the plausible set of inter-sectoral elasticities (σ, θ, e, η),

25. This calculation misses differences in lives saved and costs incurred in 2021, outside the simulation window.

where σ is the elasticity of substitution in consumption, θ is the elasticity of substitution across intermediates in production, e is the elasticity of substitution between value added and intermediates in production, and η is the elasticity of substitution between capital and labor in production. We consider low elasticities given the short horizons involved. When $(\sigma, \theta, e, \eta) = (1, 1, 1, 1)$, so that Hulten's theorem applies globally, the reduction in real GDP is 7.3 percent. When $(\sigma, \theta, e, \eta) = (0.95, 0.001, 0.7, 0.5)$, the reduction in real GDP is 7.9 percent. When $(\sigma, \theta, e, \eta) = (0.7, 0.001, 0.3, 0.2)$, the reduction in real GDP is 9.5 percent. Finally, when $(\sigma, \theta, e, \eta) = (0.5, 0.001, 0.3, 0.2)$, the reduction in real GDP is 10.1 percent. Hence, empirically plausible complementarities in consumption and in production can amplify real GDP losses, relative to what we have reported, by somewhere between 10 and 40 percent.

VII. Discussion

The modeling presented here goes beyond what is in the literature by incorporating an age-based SEIQRD model into a sectoral economic model with multiple, explicitly specified NPIs, calibrated and estimated to current US conditions using the most recently available data. Still, multiple caveats are in order. One is that the situation differs by state, with Northeastern states seeing a sharp decline in infections and deaths in May through July 2020, but other parts of the United States seeing expansions in infections and deaths. The national modeling here abstracts from these differences. In addition, there is considerable uncertainty over some key epidemiological parameters, such as the infection-fatality ratio. Additional simulation results in the online appendix explore the sensitivity of the modeling results to some of the key epidemiological parameters. Although numerical values differ—for example, under all control scenarios deaths are higher if a higher value of the IFR is assumed—the conclusions from section VI are robust.

For convenience, we have called the decision maker in the model the governor. This is a simplification of a complex decision-making environment in which federal guidelines, state requirements and guidelines, local implementation, and individual decisions combine to influence the spread of the virus. There is a compelling body of work that much of the decline in economic activity in March and April was not directly caused by government intervention but instead was an endogenous self-protective response by consumers and, similarly, that official reopenings had limited if any direct causal effect on spending (Bartik and others 2020; Gupta, Simon, and Wing 2020). If so, one might think of consumers as more akin to our

slow governor. Under this interpretation, our results align with the reduced-form evidence that the key to reviving the economy is providing a setting in which consumers and workers are comfortable returning to economic activity, that is, in which deaths are low and declining.

Our governor in these simulations used a backward-looking PID control rule based on the CDC suggested guidelines. This differs from most of the recent economic modeling surveyed in the introduction, which investigates optimal control rules. These approaches are complementary: optimal control provides insights about how economic decisions could optimally be made; the approach here asks how various NPIs can reduce or eliminate the need for adhering to lockdowns within the context of existing economic reopening or closing plans. One issue that has not been addressed in the economics literature using optimal control is the large amount of parameter and model uncertainty, which is ignored under standard optimal control rules but is reflected in the uncertainty bands in our figures and in the online appendix. Addressing this uncertainty could be done using the tools of robust control, but that has not yet been done in combined economics-epidemiological models.[26]

The main conclusion from the simulations in section VI is that aggressive use of noneconomic NPIs can lead to a reduction in deaths and a strong economic reopening. If a second wave emerges, a second round of economic shutdowns would be both costly and ineffective, compared to noneconomic NPIs. A key noneconomic NPI is returning to phase I–level restrictions on noneconomic social activities, combined with widespread adoption of measures to reduce transmission such as masks and personal distancing. When combined with other measures, such as ramped-up testing and quarantine and enhanced protection of the elderly, especially in nursing homes, these noneconomic NPIs can provide a powerful force to control a second wave and, based on our modeling, make room for bringing the large majority of those currently not working back to work.

ACKNOWLEDGMENTS We thank Veronica De Falco, Michael Droste, Adriano Fernandes, Kathryn Holston, Stephanie Kestelman, Ed Kong, Danila Maroz, Chika Okafor, and Lingdi Xu for research assistance; Caroline Buckee, Jason Furman, James Hay, Abigail Wozniak, and Jan Eberly for discussions; and Daron Acemoglu and David Romer for comments. This research was supported by NSF RAPID Grant SES-2032493.

26. See, however, Morris and others (2020) for an example within an epidemiology-only model.

References

Acemoglu, Daron, Victor Chernozhukov, Iván Werning, and Michael D. Whinston. 2020. "Optimally Targeted Lockdowns in a Multi-Group SIR Model." Working Paper 27102. Cambridge, Mass.: National Bureau of Economic Research.

Alvarez, Fernando E., David Argente, and Francesco Lippi. 2020. "A Simple Planning Problem for COVID-19 Lockdown." Working Paper 26981. Cambridge, Mass.: National Bureau of Economic Research.

Atkeson, Andrew. 2020a. "What Will Be the Economic Impact of COVID-19 in the US? Rough Estimates of Disease Scenarios." Working Paper 26867. Cambridge, Mass.: National Bureau of Economic Research.

Atkeson, Andrew. 2020b. "How Deadly Is COVID-19? Understanding the Difficulties with Estimation of Its Fatality Rate." Working Paper 26965. Cambridge, Mass.: National Bureau of Economic Research.

Aum, Sangin, Sang Yoon (Tim) Lee, and Yongseok Shin. 2020. "Inequality of Fear and Self-Quarantine: Is There a Trade-Off between GDP and Public Health?" Working Paper 27100. Cambridge, Mass.: National Bureau of Economic Research.

Azzimonti, Maria, Allesandra Fogli, Fabrizio Perri, and Mark Ponder. 2020. "Social Distance Policies in ECON-EPI Networks." Working Paper. http://marina-azzimonti.com/wp-content/uploads/2020/07/Draft_july18.pdf.

Baqaee, David, and Emmanuel Farhi. 2019. "The Macroeconomic Impact of Microeconomic Shocks: Beyond Hulten's Theorem." *Econometrica* 87, no. 4: 1155–203.

Baqaee, David, and Emmanuel Farhi. 2020a. "Nonlinear Production Networks with an Application to the COVID-19 Crisis." Working Paper 27281. Cambridge, Mass.: National Bureau of Economic Research.

Baqaee, David, and Emmanuel Farhi. 2020b. "Supply and Demand in Disaggregated Keynesian Economics with an Application to the COVID-19 Crisis." Working Paper 27152. Cambridge, Mass.: National Bureau of Economic Research.

Bartik, Alexander W., Marianne Bertrand, Feng Lin, Jesse Rothstein, and Matthew Unrath. 2020. "Measuring the Labor Market at the Onset of the COVID-19 Crisis." In the present volume of *Brookings Papers on Economic Activity*.

Berger, David, Kyle Herkenhoff, and Simon Mongey. 2020. "An SEIR Infectious Disease Model with Testing and Conditional Quarantine." Working Paper 2020-25. Chicago: University of Chicago, Becker Friedman Institute for Economics.

Bick, Alexander, Adam Blandin, and Karel Mertens. 2020. "Work from Home after the COVID-19 Outbreak." Working Paper 2017. Federal Reserve Bank of Dallas. https://www.dallasfed.org/research/papers/2020/wp2017.

Bloom, Nicholas, James Liang, John Roberts, and Zhichun Jenny Ying. 2015. "Does Working from Home Work? Evidence from a Chinese Experiment." *Quarterly Journal of Economics* 130, no. 1: 165–218.

Boast, Alison, Alasdair Munro, and Henry Goldstein. 2020. "An Evidence Summary of Paediatric COVID-19 Literature." Blog post, September 26, Don't Forget the Bubbles. http://doi.org/10.31440/DFTB.24063.

Bodenstein, Martin, Giancarlo Corsetti, and Luca Guerrieri. 2020. "Social Distancing and Supply Disruptions in a Pandemic." Finance and Economics Discussion Series 2020-031. Washington: Board of Governors of the Federal Reserve System.

Budish, Eric B. 2020. "$R < 1$ as an Economic Constraint: Can We 'Expand the Frontier' in the Fight against Covid-19?" Working Paper 2020-31. Chicago: University of Chicago, Booth School of Business.

Chu, Derek K., Elie A. Akl, Stephanie Duda, Karla Solo, Sally Yaacoub, Holger J. Schünemann, and others. 2020. "Physical Distancing, Face Masks, and Eye Protection to Prevent Person-to-Person Transmission of SARS-CoV-2 and COVID-19: A Systematic Review and Meta-Analysis." *Lancet* 394, no. 10242: 1949–2020.

Conference Board. 2020. "A Realistic Blueprint for Reopening the Economy by Sector while Ramping Up Testing." Solutions Brief. Arlington, Va.: Committee for Economic Development of the Conference Board. https://www.ced.org/2020-solutions-briefs/a-realistic-blueprint-for-reopening-the-economy-by-sector-while-ramping-up.

Cori, Anne, Neil M. Ferguson, Christophe Fraser, and Simon Cauchemez. 2013. "A New Framework and Software to Estimate Time-Varying Reproduction Numbers during Epidemics." *American Journal of Epidemiology* 178, no. 9: 1505–12.

Dingel, Jonathan I., and Brent Neiman. 2020. "How Many Jobs Can Be Done at Home?" *Journal of Public Economics* 189, article no. 104235.

Dingel, Jonathan I., Christina Patterson, and Joseph Vavra. 2020. "Childcare Obligations Will Constrain Many Workers When Reopening the US Economy." Working Paper 2020-46. Chicago: University of Chicago, Becker Friedman Institute for Economics.

Dorèlien, Audrey M., Aparna Ramen, and Isabella Swanson. 2020. "Analyzing the Demographic, Spatial, and Temporal Factors Influencing Social Contact Patterns in the U.S. and Implications for Infectious Disease Spread." Working Paper 2020-05. Minneapolis: Minnesota Population Center, University of Minnesota. https://assets.ipums.org/_files/mpc/wp2020-05.pdf.

Eichenbaum, Martin S., Sergio T. Rebelo, and Mathias Trabandt. 2020a. "The Macroeconomics of Epidemics." Working Paper 26882. Cambridge, Mass.: National Bureau of Economic Research.

Eichenbaum, Martin S., Sergio T. Rebelo, and Mathias Trabandt. 2020b. "Epidemics in the Neoclassical and New Keynesian Models." Working Paper w27430. Cambridge, Mass.: National Bureau of Economic Research.

Farboodi, Maryam, Gregor Jarosch, and Robert Shimer. 2020. "Internal and External Effects of Personal Distancing in a Pandemic." Working Paper 27059. Cambridge, Mass.: National Bureau of Economic Research.

Favero, Carlo A., Andrea Ichino, and Aldo Rustichini. 2020. "Restarting the Economy while Saving Lives under COVID-19." Discussion Paper DP14664. London: Centre for Economic Policy Research.

Ferguson, Neil M., Daniel Laydon, Gemma Nedjati-Gilani, Natsuko Imai, Kylie Ainslie, Marc Baguelin, and others. 2020. *Report 9: Impact of Non-pharmaceutical*

Interventions (NPIs) to Reduce COVID-19 Mortality and Healthcare Demand. London: Imperial College COVID-19 Response Team.

Glover, Andrew, Jonathan Heathcote, Dirk Krueger, and José-Víctor Ríos-Rull. 2020. "Health versus Wealth: On the Distributional Effects of Controlling a Pandemic." Working Paper 27046. Cambridge, Mass.: National Bureau of Economic Research.

Gottlieb, Scott, Caitlin Rivers, Mark McClellan, Lauren Silvis, and Crystal Watson. 2020. *National Coronavirus Response: A Road Map to Reopening*. Washington: American Enterprise Institute. https://www.aei.org/research-products/report/national-coronavirus-response-a-road-map-to-reopening/.

Guðbjartsson, Daniel F., Agnar Helgason, Hakon Jonsson, Olafur T. Magnusson, Pall Melsted, Gudmundur L. Norddahl, and others. 2020. "Spread of SARS-CoV-2 in the Icelandic Population." *New England Journal of Medicine* 382, no. 24: 2302–15.

Guerrieri, Veronica, Guido Lorenzoni, Ludwig Straub, and Iván Werning. 2020. "Macroeconomic Implications of COVID-19: Can Negative Supply Shocks Cause Demand Shortages?" Working Paper 26918. Cambridge, Mass.: National Bureau of Economic Research.

Gupta, Sumedha, Kosali Simon, and Coady Wing. 2020. "Mandated and Voluntary Social Distancing during the COVID-19 Epidemic." In the present volume of *Brookings Papers on Economic Activity*.

Hall, Robert E., Charles I. Jones, and Peter J. Klenow. 2020. "Trading off Consumption and COVID-19 Deaths." Federal Reserve Bank of Minneapolis *Quarterly Review* 42, no. 1: 2–13.

Hay, James A., David J. Haw, William P. Hanage, C. Jessica E. Metcalf, and Michael J. Mina. 2020. "Implications of the Age Profile of the Novel Coronavirus." Manuscript, Harvard University.

Howard, Jeremy, Austin Huang, Zhiyuan Li, Zeynep Tufekci, Vladimir Zdimal, Helene-Mari van der Westhuizen, and others. 2020. "Face Masks against COVID-19: An Evidence Review." Preprints. https://www.preprints.org/manuscript/202004.0203/v2.

Hulten, Charles R. 1978. "Growth Accounting with Intermediate Inputs." *Review of Economic Studies* 45 no. 3: 511–18.

Jones, Callum J., Thomas Philippon, and Venky Venkateswaran. 2020. "Optimal Mitigation Policies in a Pandemic: Social Distancing and Working from Home." Working Paper 26984. Cambridge, Mass.: National Bureau of Economic Research.

Kaiser Family Foundation. 2020. "State Data and Policy Actions to Address Coronavirus." Issue Brief. San Francisco: Kaiser Family Foundation. Accessed June 21. https://www.kff.org/health-costs/issue-brief/state-data-and-policy-actions-to-address-coronavirus/.

Katz, Josh, Denise Lu, and Margot Sanger-Katz. 2020. "The Toll Since Coronavirus Struck: 266,000 More Deaths than Normal." *New York Times*, May 6 (accessed July 10, 2020). https://www.nytimes.com/interactive/2020/05/05/us/coronavirus-death-toll-us.html.

Kissler, Stephen M., Christine Tedijanto, Edward Goldstein, Yonatan H. Grad, and Marc Lipsitch. 2020. "Projecting the Transmission Dynamics of SARS-CoV-2 through the Postpandemic Period." *Science* 368, no. 6493: 860–68.

Krueger, Dirk, Harald Uhlig, and Taojun Xie. 2020. "Macroeconomic Dynamics and Reallocation in an Epidemic: Evaluating the 'Swedish Solution.'" Working Paper 27047. Cambridge, Mass.: National Bureau of Economic Research.

Lin, Zhixian, and Christopher M. Meissner. 2020. "Health vs. Wealth? Public Health Policies and the Economy during COVID-19." Working Paper 27099. Cambridge, Mass.: National Bureau of Economic Research.

Ludvigson, Sydney C., Sai Ma, and Serena Ng. 2020. "COVID-19 and the Macroeconomic Effects of Costly Disasters." Working Paper 26987. Cambridge, Mass.: National Bureau of Economic Research.

Mas, Alexandre, and Amanda Pallais. 2020. "Alternative Work Arrangements." *Annual Review of Economics* 12, no. 1: 631–58.

Mongey, Simon, Laura Pilossoph, and Alex Weinberg. 2020. "Which Workers Bear the Burden of Social Distancing Policies?" Working Paper 27085. Cambridge, Mass.: National Bureau of Economic Research.

Morris, Dylan H., Fernando W. Rossine, Joshua B. Plotkin, and Simon A. Levin. 2020. "Optimal, Near-Optimal, and Robust Epidemic Control." ArXiv:2004.02209. Ithaca, N.Y.: Cornell University.

Moser, Christian A., and Pierre Yared. 2020. "Pandemic Lockdown: The Role of Government Commitment." Working Paper 27062. Cambridge, Mass.: National Bureau of Economic Research.

Mulligan, Casey B. 2020. "Economic Activity and the Value of Medical Innovation during a Pandemic." Working Paper 27060. Cambridge, Mass.: National Bureau of Economic Research.

National Governors Association. 2020. "Roadmap to Recovery: A Public Health Guide for Governors." Washington: Author. https://www.nga.org/center/publications/health/roadmap-to-recovery/.

Poletti, Piero, Marcello Tirani, Danilo Cereda, Filippo Trentini, Giorgio Guzzetta, Giuliana Sabatino, and others. 2020. "Probability of Symptoms and Critical Disease after SARS-CoV-2 Infection. ArXiv:2006.08471. Ithaca, N.Y.: Cornell University.

Rampini, Adriano A. 2020. "Sequential Lifting of COVID-19 Interventions with Population Heterogeneity." Working Paper 27063. Cambridge, Mass.: National Bureau of Economic Research.

Rio-Chanona, R. Maria del, Penny Mealy, Anton Pichler, François Lafond, and J. Doyne Farmer. 2020. "Supply and Demand Shocks in the COVID-19 Pandemic: An Industry and Occupation Perspective." *Oxford Review of Economic Policy* 36, suppl. 1: S94–137.

Romer, Paul. 2020. "Roadmap to Responsibly Reopen America." https://roadmap.paulromer.net/.

Salje, Henrik, Cécile Tran Kiem, Noémie Lefrancq, Noémie Courtejoie, Paolo Bosetti, Juliette Paireau, and others. 2020. "Estimating the Burden of SARS-CoV-2

in France." *Science* 369, no. 6500: 208–11. https://science.sciencemag.org/content/early/2020/05/12/science.abc3517/tab-pdf.

Stock, James H. 2020. "Data Gaps and the Policy Response to the Novel Coronavirus." Working Paper 26902. Cambridge, Mass.: National Bureau of Economic Research.

Tian, Liang, Xuefei Li, Fei Qi, Qian-Yuan Tang, Viola Tang, Jiang Liu, and others. 2020. "Calibrated Intervention and Containment of the COVID-19 Pandemic." ArXiv:2003.07353. Ithaca, N.Y.: Cornell University. https://arxiv.org/pdf/2003.07353.pdf.

Towers, Sherry, and Zhilan Feng. 2012. "Social Contact Patterns and Control Strategies for Influenza in the Elderly." *Mathematical Biosciences* 240, no. 2: 241–49.

US Environmental Protection Agency. 2010. *Guidelines for Preparing Economic Analyses*. https://www.epa.gov/sites/production/files/2017-09/documents/ee-0568-22.pdf.

van den Driessche, Pauline. 2017. "Reproduction Numbers of Infectious Disease Models." *Infectious Disease Modelling* 2, no. 3: 288–303.

Verity, Robert, Lucy C. Okell, Ilaria Dorigatti, Peter Winskill, Charles Whittaker, Natsuko Imai, and others. 2020. "Estimates of the Severity of COVID-19 Disease." MedRxiv. https://www.medrxiv.org/content/10.1101/2020.03.09.20033357v1.

Vogel, Gretchen, and Jennifer Couzin-Frankel. 2020. "Should Schools Reopen? Kids' Role in Pandemic Still a Mystery." *Science*, May 4. https://www.sciencemag.org/news/2020/05/should-schools-reopen-kids-role-pandemic-still-mystery.

White House, Centers for Disease Control and Prevention, and Food and Drug Administration. 2020. "Testing Blueprint: Opening Up America Again." Washington: Authors. https://www.whitehouse.gov/wp-content/uploads/2020/04/Testing-Blueprint.pdf.

Yang, Rongrong, Xien Gui, and Yong Xiong. 2020. "Comparison of Clinical Characteristics of Patients with Asymptomatic vs Symptomatic Coronavirus Disease 2019 in Wuhan, China." *JAMA Network Open* 3, no 5.